doi: 10.12029/gc20190613

赵衡,张进,李岩峰,曲军峰,张北航,张义平,云龙,王艳楠. 2019. 内蒙古狼山地区新生代断层活动特征:对正断层生长的限定[J]. 中国地质, 46(6): 1433−1453.

Zhao Heng, Zhang Jin, Li Yanfeng, Qü Junfeng, Zhang Beihang, Zhang Yiping, Yun Long, Wang Yannan. 2019. Characteristics of Cenozoic faults in Langshan area, Inner Mongolia: Constraint on the development of normal faults[J]. Geology in China, 46(6): 1433−1453(in Chinese with English abstract).

内蒙古狼山地区新生代断层活动特征:对正断层生长的限定

赵衡[1],张进[1],李岩峰[2],曲军峰[1],张北航[1],张义平[3],云龙[4],王艳楠[5]

(1.中国地质科学院地质研究所,北京 100037;2.中国地震应急搜救中心,北京 100049;3.中国地质科学院,北京 100037;4.核工业北京地质研究院,北京 100029 5.河北工程大学地球科学与工程学院,河北 邯郸 056000)

提要: 阿拉善地块东北缘的狼山地区新生代发育有3期构造,分别为中新世NW−SE向挤压形成的逆断层,NNE向挤压形成的左行走滑断层以及晚新生代NW−SE向伸展形成的高角度正断层。结合阿拉善地块东缘的新生代构造,认为狼山地区新生代断层的活动与青藏高原东北缘的逐步扩展、应力场逐渐调整有关。狼山山前正断层目前是一条贯通的断层,其演化基本符合恒定长度断层生长模型,断层中间部位滑动速率最大,向断层两侧逐渐递减。从不同方法得出的滑动速率来看,进入全新世以来,断层滑动速率有逐渐变小的趋势。结合阿拉善地块内部及东缘断层震源机制解以及断层的几何学、运动学特征,认为河套—吉兰泰盆地和银川盆地属于两个性质不同的伸展盆地,两者通过构造转换带相连,转换区内断层表现为右行走滑。转换区5级以上地震可能是受区域性NE−SW向挤压,近南北向右行断层活动的表现。

关 键 词: 狼山;正断层;断层生长;阿拉善; 青藏高原; 地质调查工程

中图分类号: P542 **文献标志码:** A **文章编号:** 1000−3657(2019)06−1433−21

Characteristics of Cenozoic faults in Langshan area, Inner Mongolia: Constraint on the development of normal faults

ZHAO Heng[1], ZHANG Jin[1], LI Yanfeng[2], QÜ Junfeng[1],
ZHANG Beihang[1], ZHANG Yiping[3], YUN Long[4], WANG Yannan[5]

(1. *Institute of Geology, Chinese Academy of Geological Sciences, Beijing,* 100037*, China;* 2. *National Earthquake Response Support Service, Beijing, 100049, China;* 3. *Chinese Academy of Geological Sciences, Beijing,* 100037*, China;* 4. *Beijing Research Institute of Uranium Geology, Beijing,* 100029*, China;* 5. *School of Earth Science and Engineering, Hebei University of Engineering, Handan* 056000, *Hebei, China*)

收稿日期: 2018−05−23;**改回日期:** 2019−07−12

基金项目: 国家自然科学基金(41572190)、国家重点基础研究发展计划(2017YFC0601301)和中国地质调查局项目(DD20190004)联合资助。

作者简介: 赵衡,男,1990年生,博士生,构造地质专业;E−mail:skzhaoheng@126.com。

通讯作者: 张进,男,1973年生,研究员,博士生导师,长期从事阿拉善周缘构造地质研究;E−mail: zhangjinem@sina.com。

Abstract: The Langshan area, located on the northeastern margin of the Alxa block, was subjected to 3 deformation stages during the Cenozoic, which produced thrust faults formed by NW−SE compression in the late Miocene, left−lateral strike-slip faults caused by NNE compression and active normal faults in the late Cenozoic. Based on peripheral Cenozoic structures around the eastern Alxa margin, the authors infer that these Cenozoic faults were related to the gradual propagation of northeast Tibetan Plateau and the readjustment of the stress field. The Langshan piedmont fault zone is now at a stage of linkup, which is compatible with the constant-length fault model with the highest slip rate in the central part. The slip rate from Holocene seems to tend to become lower relative to the slip rate since late Pleistocene. Combined with the focal mechanisms as well as geometries and kinematics of faults in and around the Alxa block, the authors tentatively propose that the Hetao−Jilantai basin and the Yinchuan basin are two different extensional basins linked by a transfer zone, in which nearly NNE−trending dextral faults are developed. The M*w* >5 earthquakes within the transfer zone probably occurred on the steep dextral faults as the result of regional SW−NE compression.

Key words: Langshan; normal faults; fault growth; Alxa; Tibetan Plateau; geological survey engineering

About the first author: ZHAO Heng, male, born in 1990, doctor candidate, majors in structural geology; E−mail: skzhaoheng@126.com.

About the corresponding author: ZHANG Jin, male, born in 1973, supervisor of doctor candidates, mainly engages in the study of structural geology in and around the Alxa region;E−mail: zhangjinem@sina.com.

Fund support: Supported by National Natural Science Foundation of China (No. 41572190), National Key Research and Development Program of China from Ministry of Science and Technology (No. 2017YFC0601301) and China Geological Survey (No. DD20190004).

1 引 言

新生代以来印度板块与欧亚板块的持续碰撞对欧亚大陆产生深远影响,青藏高原东北缘作为高原向北东扩展的最前缘,对于理解高原扩展机制和变形演化过程起到关键作用。高原东北缘对周围地区产生明显的作用,不同学者从不同角度针对碰撞远程效应的影响范围和时代提出不同的观点(Burchfiel et al., 1991;Zhang et al., 1991;Meyer et al., 1998;Jolivet et al., 2001;Tapponnier et al., 2001;Fang et al., 2003;袁道阳等,2004;Zheng et al., 2006;Clark et al., 2010;Yin, 2010;Duvall et al., 2013;Yuan et al., 2013;Shi et al., 2015;Yu et al., 2016;郑文俊等,2016)。在高原的东北缘发育有鄂尔多斯西缘新生代断裂系统(Molnar and Tapponnier, 1975;1977;Middleton et al., 2016;雷启云等,2017),该断陷系的形成与高原扩展有关,还是与西太平洋向欧亚板块下的俯冲有关是目前的争议点(Tapponnier and Molnar, 1976, 1982;Zhang et al., 1998;张岳桥等,2006;Zhang et al., 2010;施炜等,2013;Shi et al., 2015;Liu et al., 2019;Fan et al., 2019;Liang et al., 2019)。狼山地区位于河套盆地西缘,处于鄂尔多斯地块西北缘和阿拉善地块东缘的交界处,在中生代经历了多期板内变形(Darby et al., 2007;Zhang et al., 2014),新生代以来发育活动多种性质断层系统,包括逆断层、走滑断层以及最新的正断层。这些不同性质、不同时代的断层与阿拉善周缘其他地区断层有什么联系?反映了何种构造背景?通过狼山地区新生代不同期次断层的研究有助于揭示阿拉善晚新生代构造机制。

古地震序列(Rao et al., 2016; Dong et al., 2018b)、构造地貌(Dong et al., 2018a; He et al., 2018)以及断层活动性差异(Jia et al., 2015)等研究表明狼山山前正断层是由分段断层连接到一起的,目前已经是一条贯通的正断层。断层不同部位活动性存在差异,即更新世以来断层的北东段活动性强于断层的南西段,已有断层滑动速率数据同样暗示了该特征。但是不同断层段的滑动速率差异与断层分段之间有何种对应关系?目前狼山山前正断层是否符合恒定长度演化模型(constant−length model)?本文通过对狼山新生代断层平面分布、断层的切割关系,厘定新生代不同时期断层的时空关系,划分断层的活动期次,在此基础上,对狼山正断层的滑动速率和断层分段关系进行研究结合邻区研究成果,恢复研究区晚新生代应力场转变过程,在此基础上讨论河套盆地西缘及邻区与青藏高原

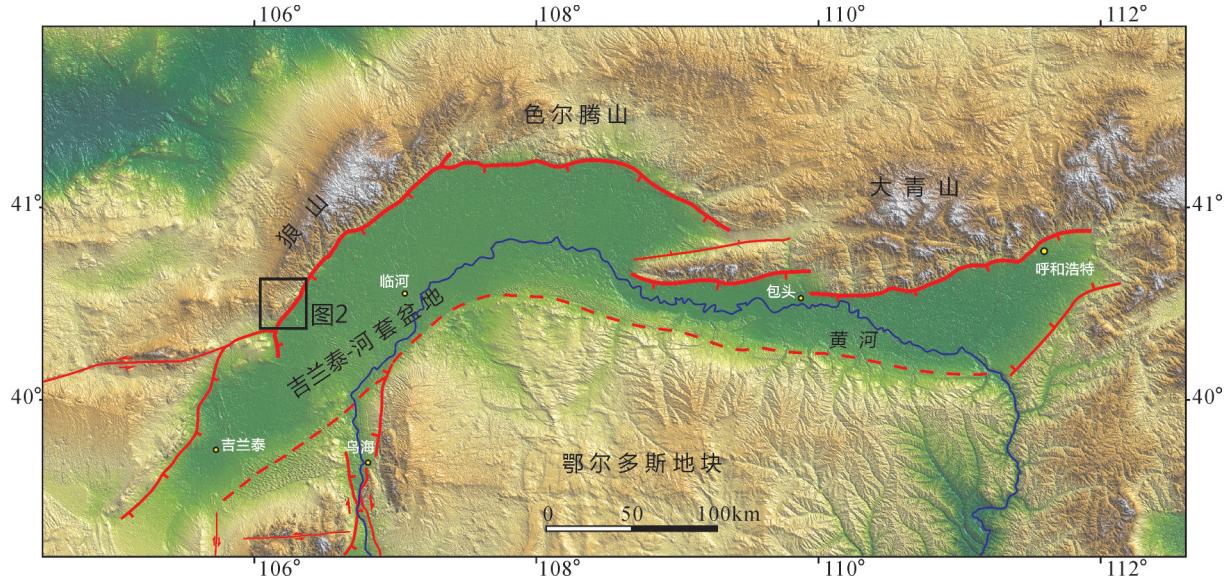

图1 河套盆地构造位置及周缘断裂分布图

Fig.1 Location of the Hetao−Jilantai Basin and the boundary faults

东北缘扩展的关系。

2 地质概况

狼山位于阴山山系的西段(图1),山脉走向北东,海拔介于1300~2400 m,中段海拔最高,向北东与色尔腾山相接,向南东与河套盆地相接,被狼山山前正断层分隔(图1)。大地构造位置上,狼山地区处于阿拉善地块和鄂尔多斯地块的边界,北侧的古亚洲洋自晚二叠世—早三叠世闭合以来(Xiao et al., 2003; Feng et al., 2013),狼山地区先后经历了三叠纪中晚期左行韧性走滑(Zhang et al., 2013),晚侏罗世NW向SE的逆冲推覆(Zhang et al., 2014; Feng et al., 2017)以及晚白垩世快速隆升(Cui et al., 2018)。新生代的构造主要受早期构造影响,在阿拉善地块和鄂尔多斯地块之间形成NE−SW向的河套—吉兰泰盆地以及近SN向的银川盆地,两个盆地以贺兰山相隔。

研究区基岩主要由古元古代叠布斯格岩群变质岩、新元古代狼山群浅变质岩(彭润民等,2010, Hu et al., 2014)、石炭纪花岗岩(Zhang et al., 2013; Dan et al., 2016)组成(图2)。叠布斯格岩群和花岗岩在三叠纪经历强烈左行剪切变形(Zhang et al., 2014),构造线走向NE,为后期构造奠定了格局。中生代地层零星出露,仅在山前残留有白垩纪陆相紫灰色碎屑岩,新生代渐新世紫红色砾岩角度不整合覆盖于早期基岩之上,向盆地方向微倾,倾角约10°(图3)。根据断层的切割关系、断层与地层的关系以及断层的多期活动,狼山地区新生代以来至少经历了3期构造活动。

狼山山前正断层同北侧的色尔腾山—乌拉山—大青山山前断层构成了河套断陷盆地的北西及北边界,是一条活动构造带(国家地震局鄂尔多斯周缘活动断裂系课题组,1988;吴卫民等,1996;江娃利,2002;冉勇康等,2003;李彦宝等,2015,图1)。狼山山前正断层缺乏大于7级地震记录,最新的古地震研究表明全新世以来的地表破裂可能贯穿全段断层(Dong et al., 2018b),地震复发周期为约2500 a(Rao et al., 2016)。

3 几何学

3.1 逆断层

狼山山脉南端基岩上盖有一套渐新世砖红色砾岩、厚层砂岩。地层角度不整合于下覆叠布斯格岩群、花岗岩以及早期白垩纪灰紫色砾岩之上,整体向南东方向倾斜,倾角约10°。狼山地区发育切穿该地层的逆断层,断层走向基本近NE,即受到基底早期构造面的控制。狼山山前正断层带的下盘局部出露逆断层露头(图4),在查斯太沟地区、代日根高勒沟口、尔驼庙南侧等地均有逆断层出露(图2)。

查斯太沟地区出露了一套由SE向NW逆冲的

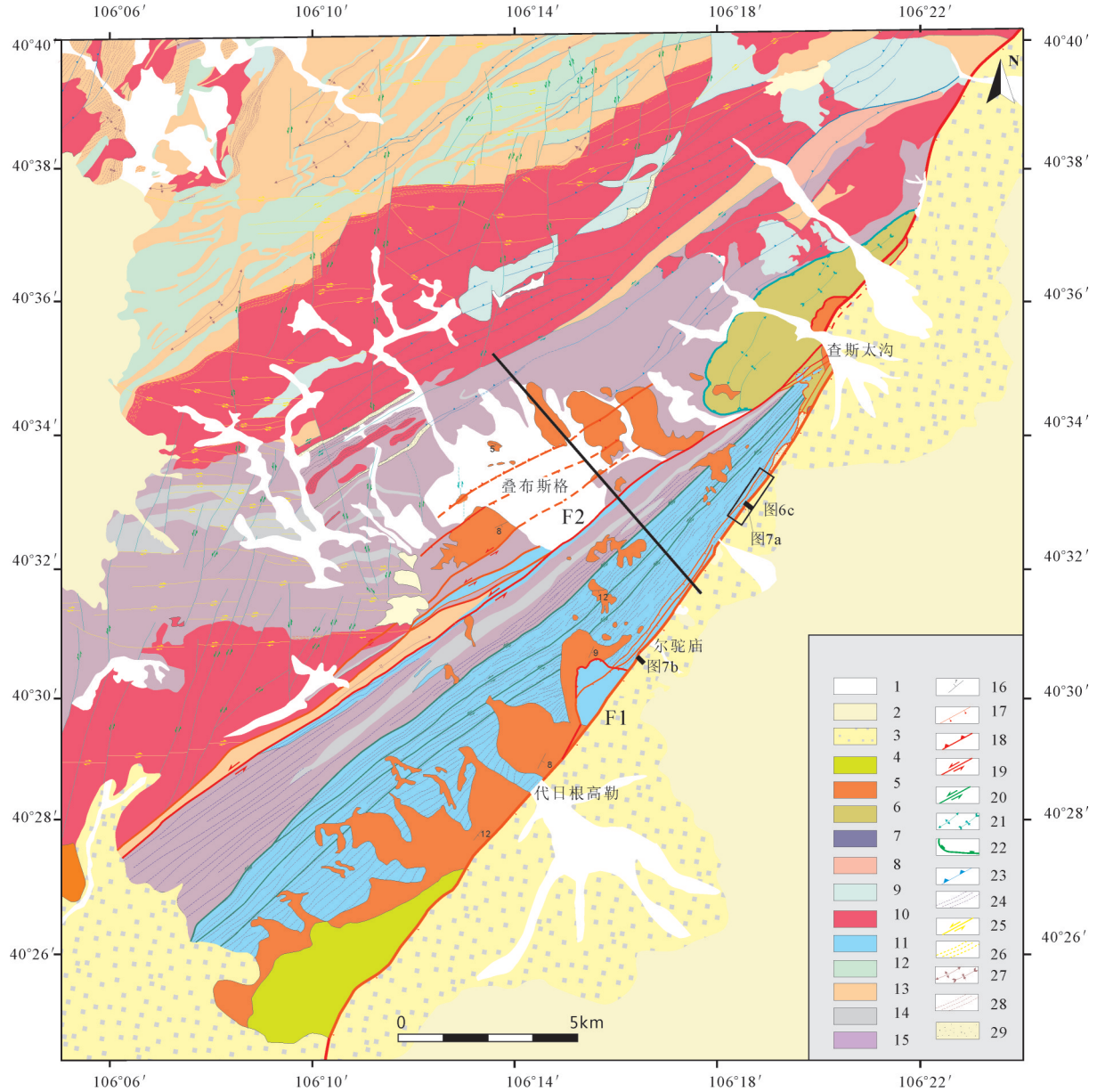

图2 狼山西南段地质图

1—全新世河道沉积; 2—第四系风成沙; 3—第四系冲洪积扇; 4—晚更新世湖相地层; 5—渐新世砾岩; 6—白垩纪砾岩; 7—三叠纪砾岩; 8—中生代花岗岩; 9—二叠纪闪长岩; 10—二叠纪二长花岗岩; 11—石炭纪花岗岩; 12—新元古代辉绿辉长岩; 13—新元古代狼山群; 14—叠布斯格岩群大理岩; 15—古元古代叠布斯格岩群; 16—渐新统产状; 17—新生代正断层; 18—新生代逆冲断层; 19—新生代走滑断层; 20—晚白垩世走滑断层; 21—早白垩世褶皱; 22—早白垩世拆离断层; 23—侏罗纪逆冲断层; 24—晚三叠世糜棱面理; 25—早三叠世走哈断层; 26—早三叠世糜棱面理; 27—晚二叠世褶皱; 28—早古生代糜棱面理; 29—断层角砾岩

Fig.2 Geological map of southwestern Langshan area

1− Holocene fluvial deposits; 2− Eolian sands; 3− Holocene alluvial fans; 4− Late Pleistocene lacustrine deposits; 5− Oligocene conglomerate; 6− Cretaceous conglomerate; 7− Triassic conglomerate; 8− Mesozoic granite; 9− Middle Permian diorite; 10− Late Permian monzogranite; 11− Carboniferous granite; 12− Neo− Proterozoic gabbro; 13− Neo− Proterozoic Langshan Group metasedimentary rocks; 14− Diebusige Group marble; 15− Paleo− Proterozoic Diebusige Group gneiss, amphibolite; 16− Attitudes of Oligocene strata; 17− Cenozoic normal fault; 18− Cenozoic reverse fault; 19− Cenozoic strike− slip fault; 20− Late Cretaceous strike− slip fault; 21− Early Cretaceous anticline and syncline; 22− Early Cretaceous detachment fault; 23−Late Jurassic reverse fault; 24−Late Triassic foliations; 25−Early Triassic foliations; 26−Early Triassic strike−slip fault; 27−Late Permian foliations; 28−Early Paleozoic foliations; 29−Fault breccia

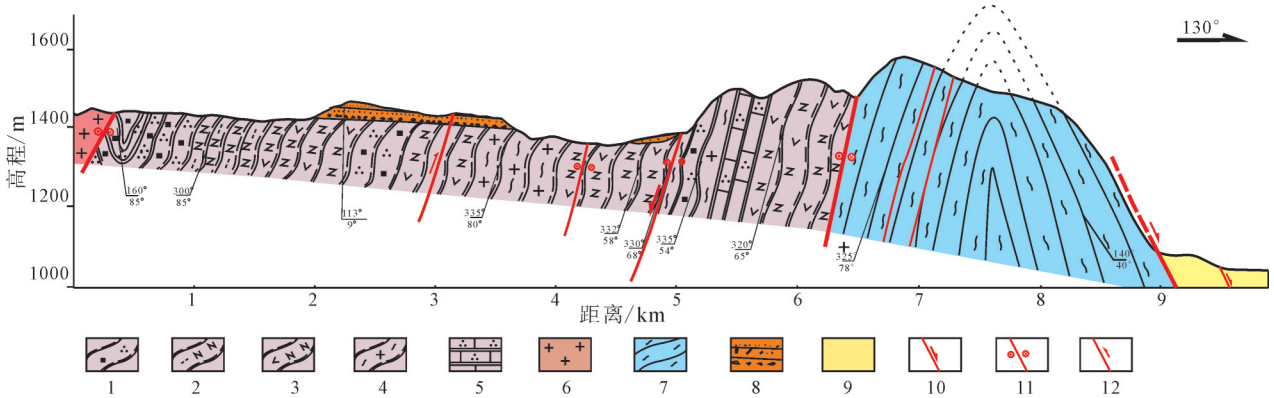

图3 图2地质剖面图(位置见图2)

1—磁铁石英岩; 2—黑云斜长片麻岩; 3—角闪斜长片麻岩; 4—花岗片麻岩; 5—大理岩; 6—二叠纪花岗岩; 7—糜棱岩; 8—渐新世砾岩; 9—全新世洪积扇; 10—正断层; 11—左行走滑断层; 12—逆断层

Fig. 3 Geological Profile(see location in Fig.2)

1−Magnetic quartzite; 2−Biotite plagioclase gneiss; 3−Hornblende plagioclase gneiss; 4−Granitic gneiss; 5−Marble; 6−Permian granite; 7−Mylonite; 8−Oligocene conglomerate; 9−Holocene alluvial fans; 10−Normal fault; 11−Left−lateral strike−slip fault; 12−Reverse fault

叠瓦状逆断层,见石炭纪花岗岩逆冲于早白垩世砾岩之上(图4a),逆断层倾向SE,倾角介于25°~40°。断层带内角砾岩发育,靠近断层核部发育一层灰白色钙质半固结断层泥,断层上盘为高度破碎的断层角砾岩,角砾成分为石炭纪花岗岩;断层下盘为白垩纪紫红色砾岩,靠近断层遭受强烈剪切(图4b)。根据断层带内剪切的透镜状角砾以及断层面上擦痕,判断该断层性质为逆冲,最大主压应力方位为NW−SE向。

尔驼庙南侧出露一逆冲断层,逆断层上盘为花岗岩,地貌上呈高耸地形,断层下盘为向SE缓倾的渐新世砾岩,靠近断层处地层被牵引褶皱,指示逆冲性质(图4c)。同时根据断层面上发育的擦痕反演得出形成逆断层的最大主压应力方位为SE−NW,即与北侧的查斯太沟地区一致。

代日根高勒冲沟口南侧,渐新世地层受逆断层影响,断层下盘地层发生褶皱,局部倒转(图4d)。逆断层面以及断层上盘被更新世河湖相地层覆盖。紧邻倒转地层东侧为逆断层,断层后缘被山前正断层切割。代日根高勒沟口北侧冲沟内见到花岗岩逆冲于渐新世砾岩之上,断层面倾角23°,断层面上发育的擦痕指示上盘向NW逆冲,两处为同一条逆断层在山前的出露。

从查斯太沟口大致沿着山体−盆地边界零星出露的逆断层、断层角砾岩以及受逆断层影响的倒转地层,共同指示了在狼山山前发育一条大型的逆断层,山前多处构造现象共同指示上盘向北西的逆冲。目前出露的是受后期断层活动破坏的残留,逆断层仅保留前缘部分。

除了在山前发育逆断层,在狼山叠布斯格盆地渐新世地层内也发育逆冲,因全新世冲洪积覆盖,逆断层露头仅在冲沟处零星出露(图4e、f)。断层走向NE,断面受基底面理控制,倾角较大,错断渐新世砾岩底部的不整合面。断层带规模小,因断层错断不整合面,视断距在几米范围内。根据断层擦痕反演得出的最大主应力指示NW−SE向的挤压(图4e),与狼山山前逆断层得出的结果一致,属于同一构造应力场。

3.2 左行走滑断层

狼山地区发育众多NE走向的走滑断层,活动时代不同(图2)。新生代活动的走滑断层依据错断新生代地层来限定。在狼山山体内部,早期走滑断层被渐新世地层覆盖,而山体两侧的走滑断层不仅切割了渐新世地层,还截切地层内逆断层。

狼山北西侧发育一条大型左行走滑断层F2(图2),F2切穿渐新世乌兰布拉格组地层(图5b, Zhang et al., 2014),表明活动时代在渐新世之后,靠近主断层,渐新世地层内部见花岗糜棱岩砾石被次级左行断裂错断,指示左行走滑性质(图5c)。F2断层面上发育多期擦痕,早期发育左行斜滑擦痕,被后期高角度倾滑擦痕叠加(图5d)。F2断层向NE延伸,在查斯太沟口南侧分成多条走滑断层,分支断层切穿

图4 狼山地区新生代逆断层及断层面解(赤平投影采用下半球投影, 后面图相同)

a—查斯太沟南侧逆断层; b—图a逆断层擦痕及断层角砾岩; c—尔驼庙南侧逆断层,下盘靠近断层处地层牵引褶皱;d—代日根高勒沟口南侧逆断层,下盘地层褶皱倒转;e~f—叠布斯格盆地内叠布斯格岩群逆冲于渐新世地层之上,断层机制解指示NW-SE向挤压

Fig .4 Reverse faults and fault-plane solutions in Langshan area (The stereographic projection is lower hemisphere projection, the same in the following figures)

a-Reverse fault on the south side of Chasitai valley; b-Fault breccia and striations in Fig. 4a; c-Reverse fault on the south side of Ertuomiao; d-Overturned strata on the south side of Dairigengaole valley, the reverse fault cut by high angle normal fault; e, f- Reverse fault in Diebusige Basin, showing nearly NW-SE compression

早期叠瓦状逆断层(图5a)。左行分支断层面上的擦痕与山体西侧主断层F2擦痕方位一致,得出的最大主应力方位为近南北向,限定左行走滑断层的活动在逆断层之后、正断层活动之前。狼山山前同样发育该期左行走滑断层,断层面受糜棱岩面理控制,断层面上见大量擦痕,断层两侧的节理受到左行走滑的影响,发生褶皱(图5e)。

3.3 正断层

活动正断层是控制狼山山脉和河套盆地的边界断层,断层向NE延伸到狼山山脉北段东乌盖沟附近,与色尔腾山山前正断层相接,长度约160 km。狼山山前正断层地貌上呈良好的线性构造,发

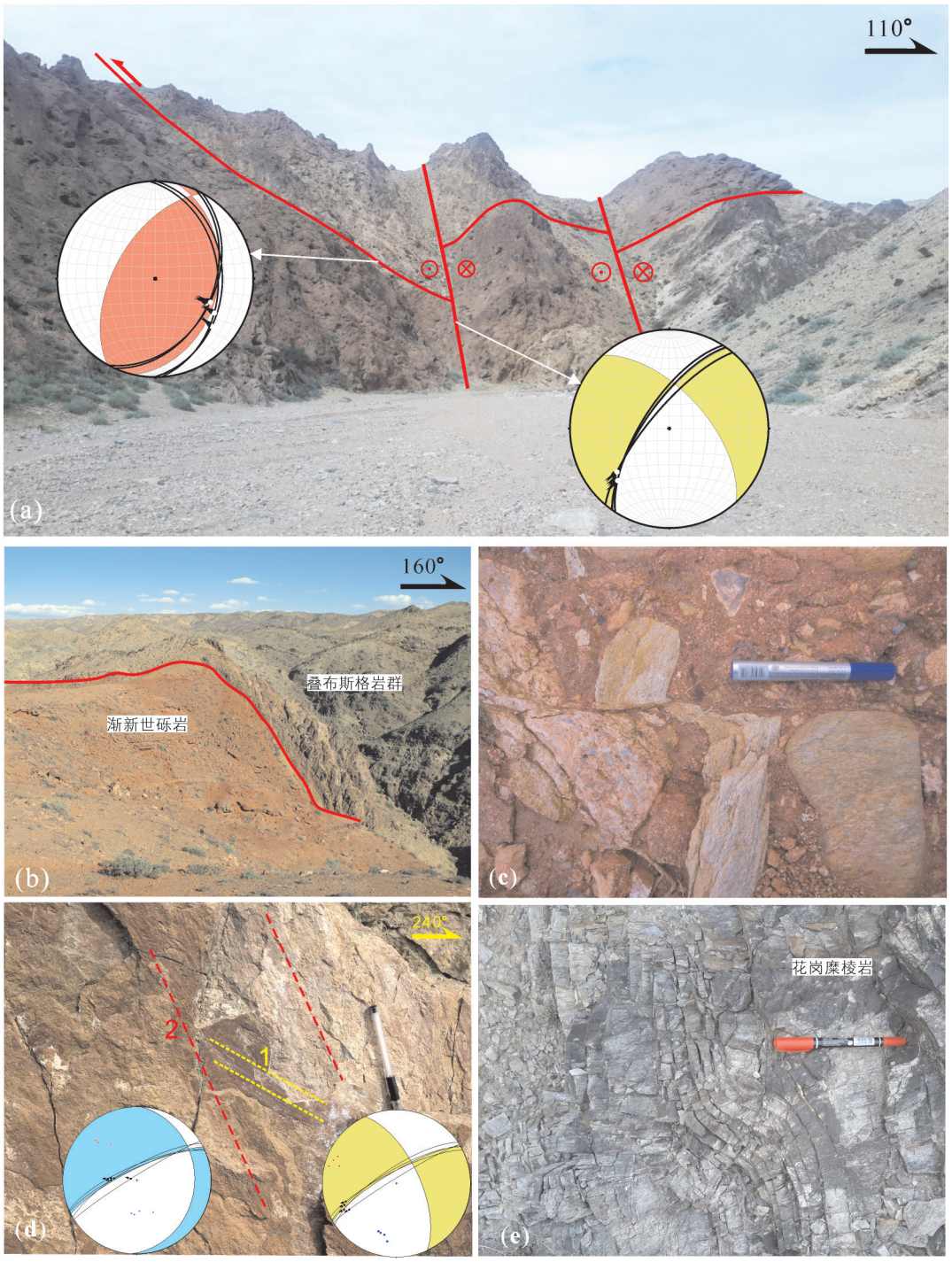

图5 狼山地区新生代左行走滑断层

a—左行走滑断层切割早期逆断层; b—左行逆断层F2,分隔渐新世断层和叠布斯格岩群; c—渐新世砾岩内部砾石被左行错断; d—F2主断层面上发育的两期擦痕,早期左行斜滑(黄色虚线)被晚期正断擦痕(红色虚线)切断; e—狼山山前糜棱岩内部左行走滑引起节理面弯曲

Fig.5 Cenozoic left-lateral strike-slip fault in Langshan area

a-Left-lateral strike-slip faults cut through reverse faults; b-Left-lateral strike-slip fault F2 separating the Wulanbulage Formation and the Diebusege Group; c-Sheared pebble in Oligocene strata showing left strike movement; d-Two stages of striations on F2, the normal oblique-slip striation (red dash line) cutting the sinistral slip striation (yellow dash line); e-Curved joints in mylonite indicating sinistral shear in Langshan piedmont area

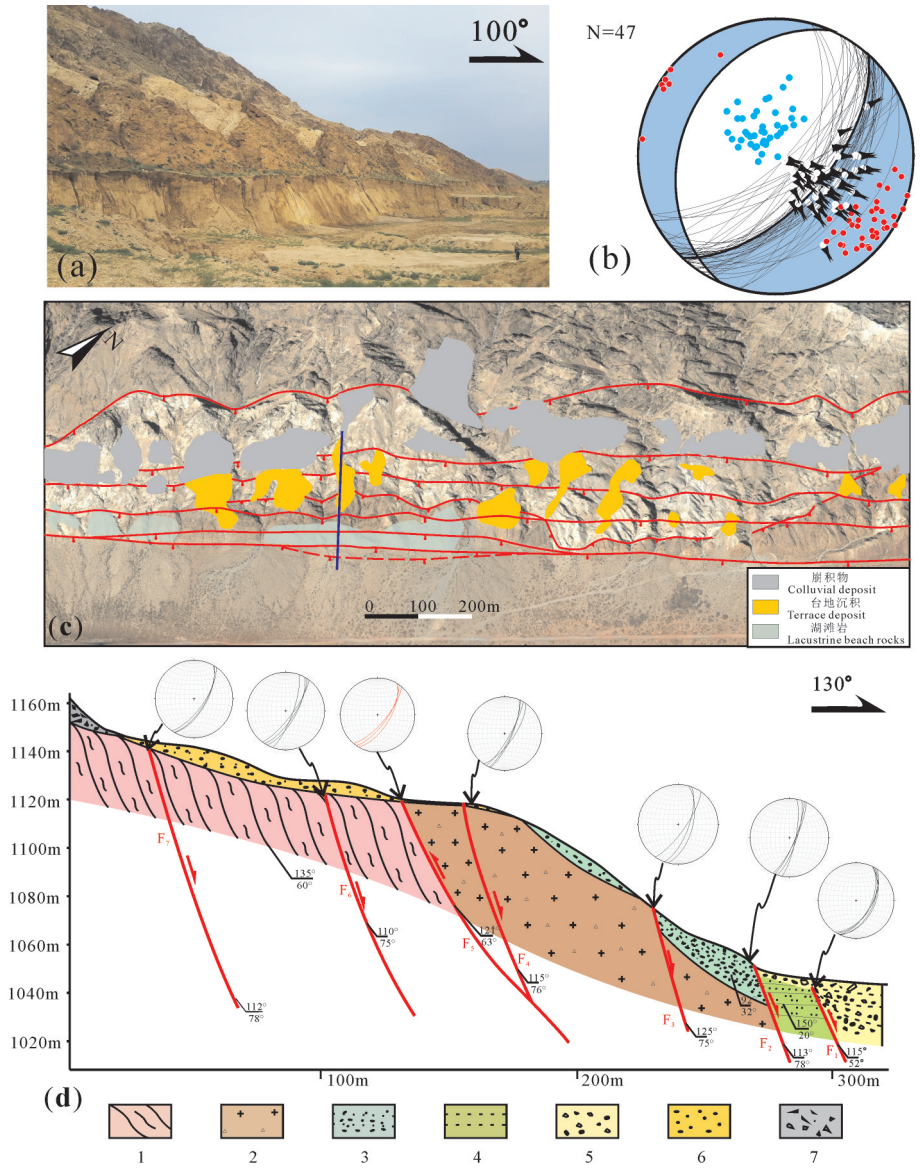

图6 狼山山前正断层带结构

a—山前正断层带外貌;b—断层面擦痕反演得出最小主应力方位为NW-SE向;c—查斯太沟南侧断层带(位置见图2);
d—图c剖面揭示断层带结构,多条阶梯状断层,最新活动断层向盆地方向迁移
1—糜棱岩;2—断层角砾岩;3—湖滩岩;4—晚更新世湖相细砂;5—全新世冲积;6—基座台地;7—崩积物

Fig. 6 Structures of Langshan piedmont fault zone

a−Photograph of piedmont normal fault; b−Fault-plane solutions suggesting NW-SE extension; c−Plan view of fault zone on the south side of Chasitai area (see Fig. 2 for location); d—Fault profile in Fig. 6c, note the fault migrated toward the basin
1−Mylonite; 2−Fault breccia; 3−Lacustrine beach rocks; 4−Late Pleistocene lacustrine fine sand;
5−Holocene alluvial fan; 6−Base terrace; 7−Colluvial deposits

育多级断层崖(图6a),山前发育多级地貌面(图6c)。从断层的几何结构来看,狼山山前发育多条正断层,构成一条沿走向宽度不等的断层带,基岩和盆地内部都发育断层,基岩内部远离盆地方向的断层被台地面上沉积覆盖,而最新活动的正断层位于盆地边缘,切断晚更新世—全新世沉积(图6d)。这与色尔腾山前正断层扩展规律类似(吴卫民等,1996)。狼山山前断层面走向集中在NE35°~40°,倾角集中在45°~75°。擦痕统计表明,山前正断层接近正倾滑,有微小的左行走滑分量,指示近NW-SE向的伸展,与区域上地应力测量、震源机制解得出的结果一致(图6b)。

4　年代学

狼山前缘正断层被现代冲洪积扇覆盖,山前冲沟揭露出最新活动断层(图7,位置见图2)。断层下盘下部为晚更新世黄绿色湖相砂质沉积,未胶结,层理发育。断层向上被全新世冲积扇覆盖,在冲积扇内的砂质透镜体内采集光释光样品,样品的前处理在中国地震局地壳应力研究所地壳动力学重点实验室完成。在实验室内弱红光下,去除钢管两端可能曝光、污染的部分,保留中心部位的样品供等效剂量测定。从中取出约20 g测定含水量和饱和含水量,之后将样品烘干充分研磨,直至全部通过63 μm的筛子,供测定样品中U、Th、K含量U、Th、K含量在核工业北京地质研究所用ELEMENT等离子体质谱分析仪测定。细颗粒样品和粗颗粒样品分别采用单片再生法(SAR, Murry et al., 2003)和简单多片再生法(SMAR, 王旭龙等,2005)进行测试, 光释光辐照和信号测量均在中国地震局地壳应力研究所地壳动力学重点实验室的丹麦Risoe DA−20−C/D型光释光自动测量系统上完成,测试结果见表1。

根据测年结果,断层上盘层位样品T20年龄为(2.66±0.32)ka,所处层位未被错断,下部层位样品T21年龄(3.62±0.4)ka,顺层延伸被断层错断,说明在2.66~3.62 ka有过一次古地震事件。由图7b可以看出,断层上盘地表以下约半米厚为棕灰色冲积,而下部为紫红色冲积层,砾石比例明显增多,两个层位颜色、砾石含量的变化界面与最新一次古地震事件吻合。Rao et al. (2016)在该露头北侧10 km处通过^{14}C年龄限定4.41~3.06 ka有一次古地震事件。结合该露头断层活动年龄,如果属于同一次地震事件,该古地震事件发生在3.62~3.06 ka。

5　讨　论

5.1　狼山新生代以来的活动期次及构造背景

从以上各断层性质、断层间切割关系可以看出:卷入逆断层的最新地层为渐新世砾岩,左行走滑断层切割了逆断层(图5a),同时在走滑断层面上发育的高角度倾滑擦痕指示后期叠加了高角度正断层(图5d)。因此在狼山地区发育了中晚新生代3期构造,分别是渐新世之后NW−SE向挤压产生的逆断层,NNE−SSW向挤压产生的左行走滑断层以及最新的NW−SE向伸展产生的正断层系统。三种性质的断层走向基本一致,呈NE−SE向延伸,主要受基底早期构造控制。中生代,尤其是晚三叠世的左行韧性走滑奠定了研究区的构造线方向,早期构造面被后期利用,体现了构造继承性。

除了狼山地区发育有逆断层,在阿拉善地块东缘的其他地区,例如贺兰山西缘也发育有挤压构造,卷入的最新地层为中新世,根据贺兰山南缘的吉井子盆地中新世同沉积构造,推测该期挤压变形的时代为中新世中晚期(Liu et al., 2019; 赵衡等,2019a)。这期挤压事件可能是受到青藏高原向北的推挤,阿拉善地块向东挤出,在地块东缘产生的一期挤压构造,狼山地区逆断层可能是该期事件在东缘的表现。随着青藏高原前缘向NE向扩展,陇中盆地遭受NE向强烈挤压,海原断裂开启活动,阿拉善地块南缘受到南侧NE方向的挤压,在块体内部早期NE向构造带基础上形成左行走滑断层。进入

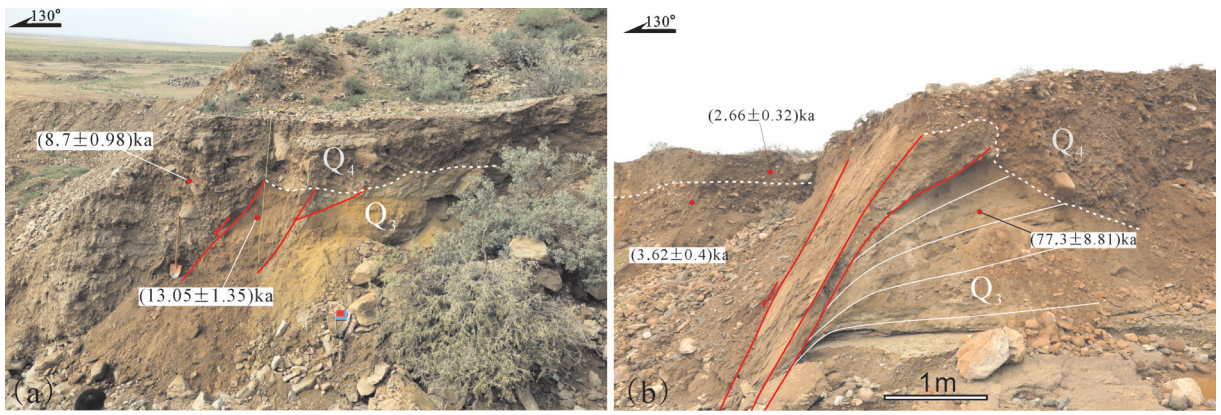

图7 狼山山前断层带前缘断层结构及光释光样品分布(位置见图2)

Fig. 7 Geometries of frontal piedmont fault zone and OSL sample locations(see Fig. 2 for location)

上新世以来，高原东北缘应力场主压应力方位发生顺时针旋转，阿拉善地块与鄂尔多斯地块之间的河套盆地和银川盆地迅速沉降，边界正断层强烈活动，盆地内沉积了巨厚的上新世地层（国家地震局鄂尔多斯周缘活动断裂系课题组，1988）。

高原东北缘的宁夏南部地区发育广泛的新生代盆地，大量研究表明高原逐渐扩展并影响到该区新生代盆地，而且经历了不同的演化阶段（Zhang et al., 2010; Wang et al., 2013; Shi et al., 2015; Lei et al., 2016; Liu et al., 2019）。狼山地区山前正断层发育之前以左行走滑活动为主，从擦痕统计的结果表明山前正断层仍有微小的左行走滑分量，说明狼山山前断层经历了从左行走滑到伸展正断的演化过程。

5.2 狼山山前正断层演化

狼山山前正断层已是一条贯通的正断层带（Dong et al., 2018a），已有不少学者通过探槽、山前河流阶地以及其他方法获得晚更新世以来的山前断层滑动速率。与河套断陷北缘的色尔腾山—乌拉山—大青山断裂相比，狼山地区滑动速率数据还十分缺乏，而且不同方法不同学者得出的结果差异较大（Shen et al., 2016; Dong et al., 2018b）。狼山山前断层带经历了长时间演化，研究表明山前断裂是由多条分段断层连接而成（He et al., 2018; Dong et al., 2018a; 赵衡等，2019b）。目前对正断层的认识有两种端元模型，一种是断层扩展模型（propagating fault model），另一种为断层恒定长度模型（constant-length fault model）。前者在断层断距增加的同时断层长度也在增加，后者是先达到断层相应的长度，断距再快速增加。自然界断层以及实验模拟的断层在形成、扩展、连接的过程中包括以上两个阶段(Rotevatn et al., 2019)。断层发育早期符合断层扩展模型，通过断层端部扩展、分段断层连接的方式使断层长度在短时间内迅速增大，随后断层演化符合恒定长度模型，表现为断层长度的有限增长或者停滞生长，而断距快速累积(Rotevatn et al., 2019)，即先获得一定的断层长度，再累积位移。为了检验狼山山前断层是否进入了后一断层演化阶段，笔者采用Cowie et al.(2001)提出的方法，根据已知某一段断层的参数（如断距、滑动速率等），求取断层不同位置的相关参数。

根据大量实例，单条断层符合$d_1=\lambda L_1$经验公式(Rotevatn et al., 2019)，其中d_1为单条独立演化断层中间部位断距，L_1为断层长度，系数λ的范围在0.001~0.1（Schultz, 1997）。多条断层连接成一整条断层后，L_2为多条断层连接后的总长度，整条断层与小规模的单条断层类似（图8a）。但是断层中间部位断层断距还处在单独分支断层的范围内，贯通后的断层长度迅速增加，进入恒定长度断层演化阶段。断层积累位移需要满足断层中间部位的断距为最大值，向断层端部断距之间减小。假设单条断层L_1中间部位位移随时间的斜率设为μ，则多条断层连接后长度达到L_2，断层中间部位的斜率为$\mu(L_2/L_1)$，也就意味着同一时间段内断层中间部位的断层滑动速率高于两侧（图8b），使断层的位移-长度曲线达到断层中间最大，断层端部最小的“半椭圆”理想曲线（图8a）。为了简化，把断层位移曲线看作一个三角形，断层的中间部位断距向断层端部线性递减，对于某一个断层l_i，定义参数$E_i=2R_i/l_i$，其中R_i是某一段断层中间点与总断层最近端部的距离，l_i为分段断层的长度，断层两端处两条分支断层$E=1$，而断层其他部位的$E>1$（图8c）。根据分段断层中间部位的E值近似代替整个分段断层，如果知道某一段断层的滑动速率或者垂直位移量，根据每条分段断层的E_i可求出断层其他段的滑动速率或者垂直位移。

该方法要求根据各种标志划分出分段断层，即寻找断层分段的标志，断层分段包括多种：几何学分段、断层结构分段、断层活动性分段以及断层的破裂分段（丁国瑜，1995）。几何学分段是依据断层

表1 狼山山前正断层带样品光释光年龄及其参数

Table 1 Ages of the OSL samples in Langshan piedmont fault zone

实验编号	野外编号	U/(μg/g)	Th/(μg/g)	K/%	环境剂量率/(Gy/ka)	测试粒径/μm	测试方法	等效剂量/Gy	年龄/ka
17-OSL-17	T20	1.64	5.25	2.88	4.22	4~11	SMAR	11.23±0.75	2.66±0.32
17-OSL-18	T21	1.58	5.11	2.79	4.09	4~11	SMAR	14.81±0.73	3.62±0.40
17-OSL-21	T54	1.97	4.26	2.36	3.71	4~11	SMAR	32.24±1.70	8.70±0.98
17-OSL-19	T23	0.96	2.17	1.94	2.36	90~125	SAR	182.66±10.00	77.30±8.81
17-OSL-20	T51	1.56	3.07	2.12	2.74	90~125	SAR	35.73±0.98	13.05±1.35

的分布排列几何学特征,结构分段考虑断层带内及两盘岩性地层结构特征差异,断层活动性分段是依据断层长期以来活动性差异的分段,而断层的破裂分段则是综合了前面3种分段,与地震断裂破裂紧密相关。

狼山目前是一条贯通断层,根据地貌学参数,例如河流纵剖面形态、高程积分、流域盆地形态以及山前弯曲度分析等结果来看,断裂下盘的抬升和河流的下切还处于非均衡状态,即断层下盘山体仍在持续快速抬升阶段(Dong et al., 2018a; He et al., 2018)。从断层带下盘的隆升来看,狼山山脉中段海拔最高,对应的断层断距最大,同时对应上盘临河凹陷的沉陷深度也最大,显示出断层中间部位的断距最大,断距向断层两端逐渐变小的特征,这也与世界其他地区的大型正断层类似(Dawers et al., 1993; Maniatis and Hampel, 2008)。He et al. (2018)与Dong et al. (2018a)把狼山山前断裂分为2个大段,断层在现今断层中间偏南部位连接。鉴于断层结构的复杂性,最初划分的段落可以进一步分为更小规模的次级段落(sub−segment, Manighetti, 2015; DuRoss et al., 2016),笔者在He et al. (2018)分段的基础上,结合狼山山前的基岩凸出、断层残留阶区以及断层下盘地形剖面对狼山山前的断层段进一步划分(图8),将狼山山前断裂段分为4个基本段,段落的长度从南向北分别为29 km、41 km、43 km、37 km。从南向北4个分段的增强因子E分别为1、2.41、2.74和1。

为了较好地限定断层不同段落上的滑动速率,需要选取某一段断层的滑动速率作为标准,要求该段断层有较可靠的断层滑动数据。求取断层滑动速率的方法可以通过地貌面的错动距离和地貌面的年龄获取,或者通过标志层的错断距离及地层的年龄获取。前者需要保存良好的地貌面,在狼山地区,山前正断层崖出露,上盘发育冲洪积扇,同一个地貌面在经历多次地震后被强烈改造,很难找到长时间尺度的同级地貌面;另一方面由于人为活动对山前地貌的改造,使得这一方法存在很大局限性。晚更新世期间河套−吉兰泰地区发育面积广阔的"河套−吉兰泰"古大湖,在120~100 ka期间发育最高湖水位,70~50 ka之前湖水开始大规模消退(Chen et al., 2008)。河套盆地西缘及北缘断层下盘普遍发育3~4级阶地,其中T1台地面紧邻盆地−基岩断裂,是由早全新世冲洪积砾石层组成的堆积台地,前缘多表现为断层陡坎。T2−T3级台地为基座台地,其上沉积晚更新世古大湖河湖相地层(公王斌等,2013),该层延续稳定,广泛沉积于狼山−色尔腾山山前台地之上,可作为晚更新世的标志层。大量的测年表明该河湖相地层的时代介于70~50 ka(Jia et al., 2015; 何泽新等,2015)。同一级台地面沿断层走向海拔高度不同,反映出断层下盘的差异隆升,Jia et al. (2015)通过对狼山山前河流阶地的测量表明狼山中段阶地面海拔高于南段,而河流阶地海拔可以和山前台地面很好对应。根据断层下盘湖相地层与邻近盆地内相应地层的垂直位移可计算

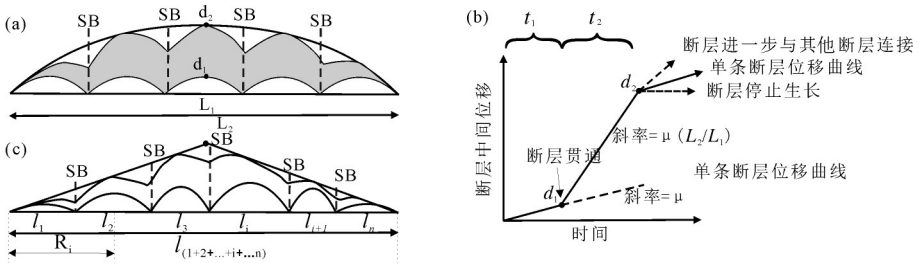

图8 a—断层位移−长度剖面,分段断层相互连接达到断层长度$L2$,之后断层以位移增加为主,长度基本不变。SB为初始断层分段边界,d_1和d_2分别为单条小断层的最大位移值以及连接后达到的最大位移值,阴影代表位移亏损区;b—断层连接后位移−时间曲线,在t_2时间段内曲线斜率变大; c—简化后的断层模型,贯通断层的滑动速率由中间向断层端部线性递减(修改自Cowie and Roberts, 2001)

Fig. 8 a−Fault displacement-length profile, fault array propagate to link with each other (fault propagating model), followed by a constant-length fault. SB marks the initial segment boundary, d_1 and d_2 are the maximum displacement of small isolated fault and the linked-up fault, the shadow area is displacement deficit; b−Displacement-time curves before and after the linkage of fault segments, note that during the t_2 , the slope is deeper than before; c−Simplified triangular shape displacement−length profile showing the displacement decrease linearly to the fault distal end (modified from Cowie and Roberts, 2001)

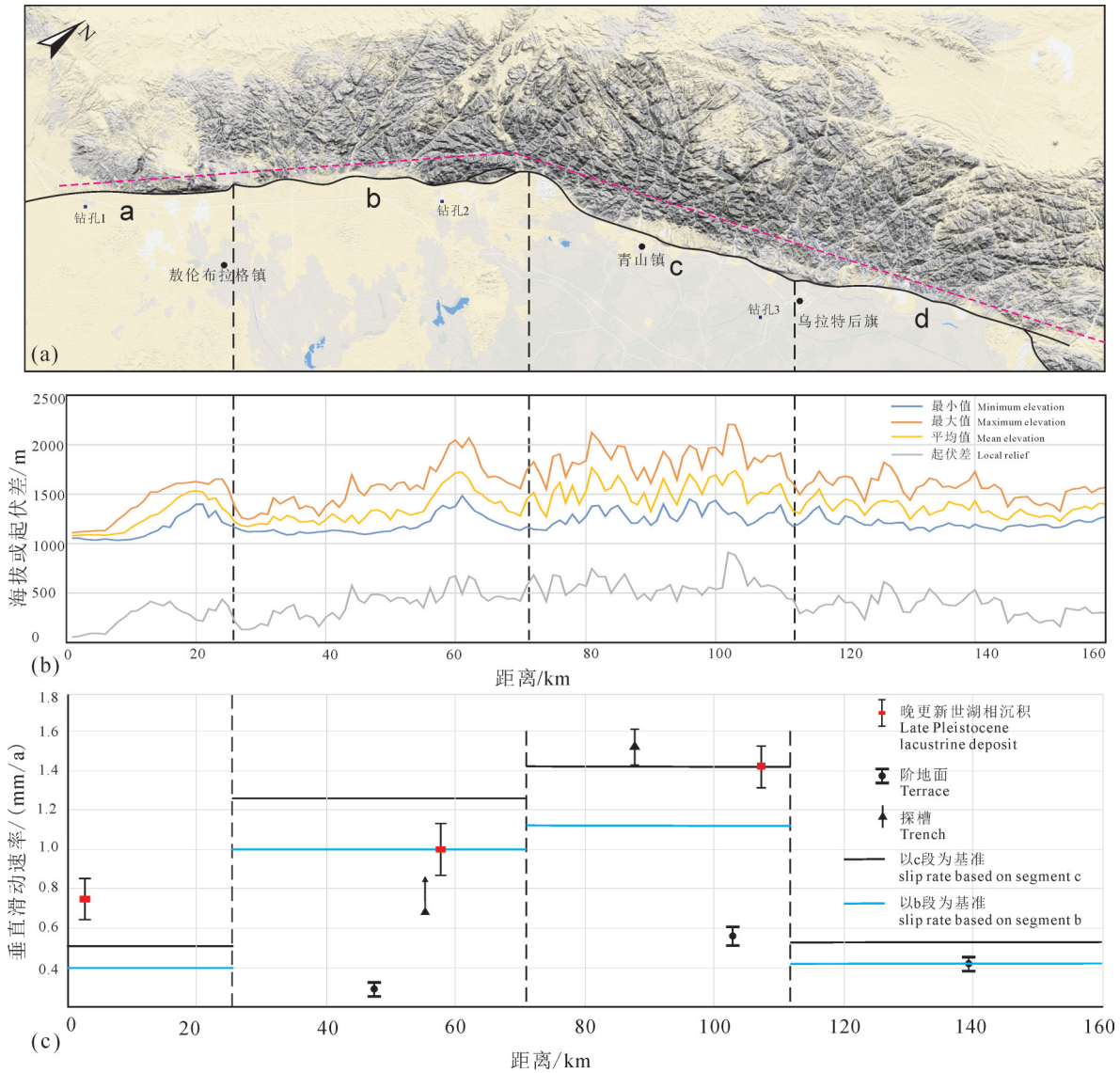

图9 狼山山前分段及各段断层滑动速率

a—狼山地貌图; b—DEM条带剖面曲线(条带宽度4 km, 条带剖面中间线对应图9a紫色虚线);
c—预测各段断层垂直滑动速率与实测值(实测数据引自董绍鹏,2016;Dong et al., 2018)

Fig.9 Fault segmentation and corresponding slip rates

a−Topography of Langshan Mountain; b−4 km wide swath topographic profile (the central line is the purple dash line in Fig. 9a);
c−Predicted slip rates compared with observed slip rates (data from Dong Shaopeng,2016; Dong et al., 2018)

晚更新世以来的断层滑动速率,该方法已经在色尔腾山地区得到应用(Zhang et al., 2017),在银川盆地北缘的乌海盆地也应用于计算断层的滑动速率(Liang et al., 2019)。

利用靠近断层的3个钻孔资料❶(图9a),通过对比邻近山前台地晚更新世湖相层海拔与钻孔揭露的对应层的海拔,得到标志层的垂直断距,因为河湖相地层的年龄集中在70 ka,取70 ka计算标志层的滑动速率(表2)。分别采用b段和c段断层的标志层滑动速率为基准,通过各断层段的E值求取其它断层段的晚更新世以来的滑动速率(图9c),同时把前人用不同方法得到的滑动速率投到图9c上。

由图9c可以看出,用b、c段的断层滑动速率得出的其它段断滑动速率,可以和钻孔数据得出的滑动速率趋势一致。即c段断层的滑动速率最高,b段次之,a段最小。用阶地面年龄计算出的年龄偏小,同时,利用探槽计算出的全新世以来的断层滑动速率(董绍鹏,2016)也偏离预测的滑动速率。多条断

表2 不同分段断层上下盘晚更新世湖相标志层海拔及滑动速率

Table 2 Elevations, depth and slip rate of the late Pleistocene lacustrine marker strata in different fault segments

断层下盘湖相层海拔/m	钻孔海拔/m	全新世厚度/m	断距范围/m	滑动速率/(mm/a)	*E*值	对应分段长度/km
1060~1075	1029	14.5	45.5~60.5	0.76±0.1	1	29.00
1060~1080	1037	37	60~80	1.0±0.14	1.24	41.00
1109~1130	1035	14.2	88.2~109.2	1.41±0.15	1.41	43.00

层连接成为一条完整断层之后,为了弥补断距亏损,需要在一定时间段内积累位移,用该方法可以较好地估算长时间尺度的断层活动速率。晚更新世以来的断层滑动速率差异可以反映出断层下盘不同部位的差异隆升,即反映为断层滑动速率的差异。此外,根据山前河流阶地和洪积台地的高程变化,晚更新世以来断层下盘抬升速率中间段大于两端,也表明下盘的差异性隆升(Jia et al., 2015; He et al., 2017)。

但是对于短时间尺度以来,如全新世以来的滑动速率,实测数据与预测值存在较大误差,除了在c段一探槽计算的滑动速率与预测的滑动速率较为一致外,其他实测值低于预测值。造成这种现象的原因一方面是实测的滑动速率是最小滑动速率,现在通过地貌测量手段获得的多级地貌面断裂陡坎前缘的高度只是断裂错动量的最小值。另一方面狼山山前存在多条分支断裂,山前冲积扇面上发育多个断层陡坎,同时盆地内部有隐伏断裂,多条断裂共同分配断层上下盘位移(Rao et al., 2018),测量得到的滑动速率可能反映了单条断层破裂行为。还有一种原因可能是全新世以来断层活动速率下降,在狼山查斯太沟口南侧一处冲沟处,由于人工开采砂土,山前局部侵蚀基准面下降,多次山洪将冲沟内全新世堆积侵蚀掉,暴露出古冲沟形态(图10)。冲沟沟口处基岩为中生代三叠纪灰紫色砾岩,现今断层位置的裂点和冲沟下游被全新世冲积扇根部埋藏(图10),说明全新世以来断层的滑动速率相对下降,上盘的堆积速率相对加快,暗示狼山山前正断层的滑动速率全新世以来降低的趋势。

5.3 阿拉善地块晚新生代构造背景

阿拉善地块南缘与青藏高原东北缘之间夹持河西走廊带,向东与鄂尔多斯地块之间被近南北向断陷盆地分隔,向北过渡到中亚造山带(图11)。阿拉善地块南边界的断层以左行逆冲为主,断裂主要发育在龙首山南北两侧,东边界受控于NNE走向的新生代盆地边界断裂。地块内部发育多条断续分布的左行走滑断层,整体呈NEE走向,断裂从狼娃山、北大山北缘经过雅布赖山前,向东可延伸到狼

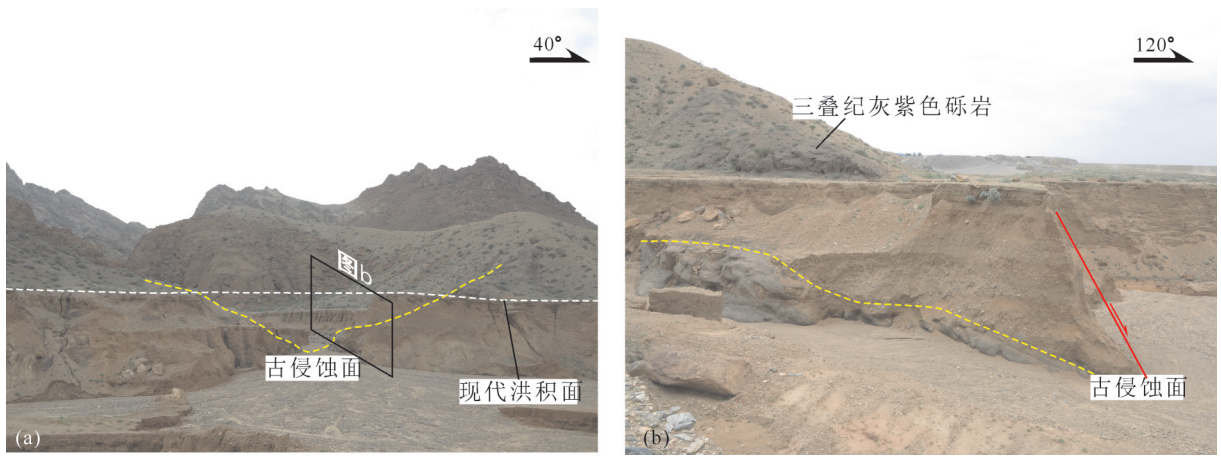

图10 人工山前开挖,局部侵蚀基准面下降,冲蚀出狼山山前断层下盘古冲沟形态

a—顺着冲冲沟方向; b—顺断层带方向

Fig.10 Paleo-valley in the footwall exposed by floods incision due to artificial digging in the hanging wall

a- Looking upstream; b-Looking along the fault strike

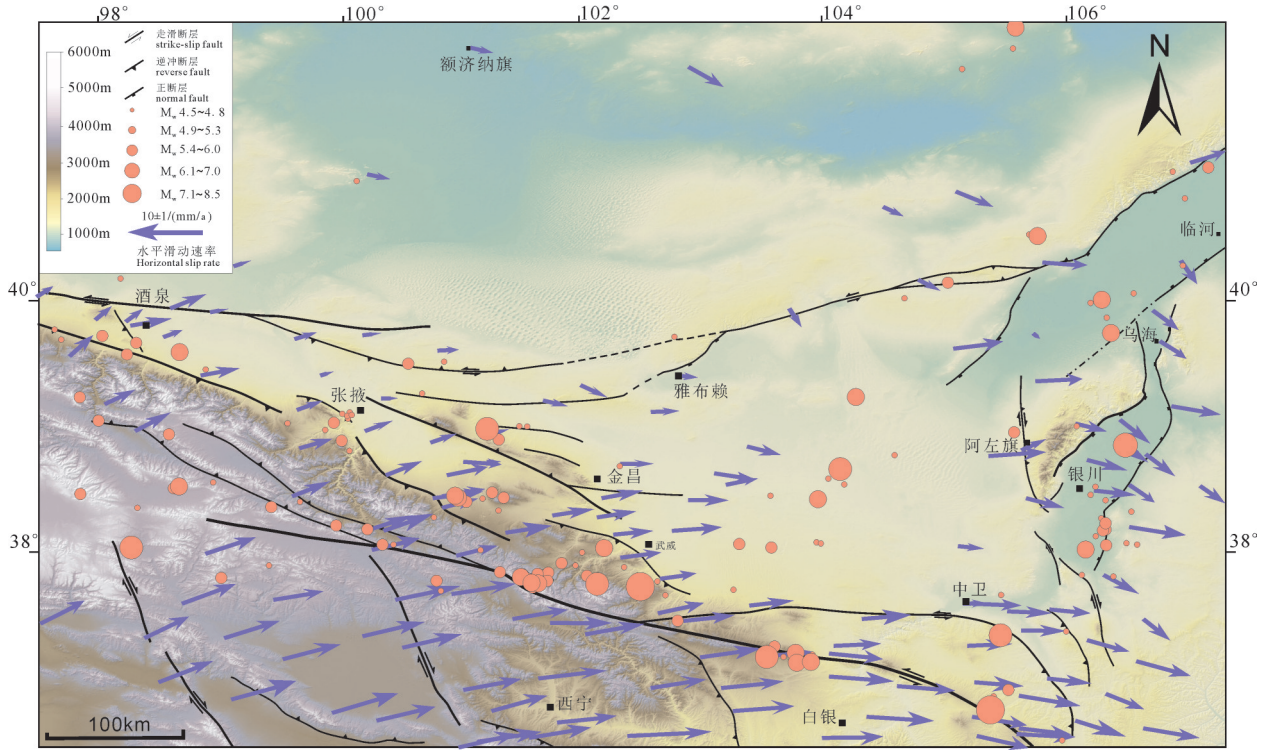

图11 阿拉善地块及邻区晚新生代断裂、GPS位移场以及大于4.5级地震分布图
（GPS位移场引自Liang et al., 2013,地震数据引自美国地质调查局）

Fig.11 Late Cenozoic faults, GPS velocity field and M*w*>4.5 earthquakes in and around the Alxa block (GPS velocity data from Liang et al., 2013; earthquakes data from USGS)

山南端。断层在左阶位置形成倾滑为主的正断层，如雅布赖断层中段（Yu et al., 2016），而在近东西向断裂为左行走滑兼逆冲，如狼娃山断裂（Yu et al., 2017）。

从阿拉善地区地震分布图（图11）中可以看出：大于4.5级以上的地震主要分布在阿拉善南缘的宽滩山—合黎山—龙首山一带以及东缘的河套—吉兰泰—银川盆地周缘。地块内部沿狼娃山—雅布赖山南缘—庆格勒图一带有零星地震分布。而阿拉善北缘少有大于4级以上地震发生，阿拉善地块北缘中亚造山带内部的戈壁—阿拉泰段（Gobi-Altai）发育密集的地震，甚至1957年分别发生8级以上地震（Choi et al., 2018）。可以看出，现今地震密集分布地区与早期地质构造有紧密联系，印度-欧亚板块碰撞导致造山带处于活化阶段（Yin et al., 1996; Cunningham, 1998, 2013）。阿拉善地块北部发育两条东西向花岗岩带，分别是北侧的宗乃山—沙拉扎山岩浆岩带以及南侧的雅布赖—巴彦诺尔公—红古尔玉林岩浆岩带，两条岩浆岩带内部结构稳定，未经历强烈的变质变形，仅在岩浆岩带的南缘发育NEE走向的韧性剪切带，可能是导致地震活动很少的原因。而阿拉善地块南部出露前寒武纪基底，岩性以花岗质片麻岩为主，形成一条走向近NWW的构造薄弱带。该构造薄弱带受到高原北缘的斜向挤压，在其持续的挤压过程中，薄弱带内早期构造面发生活动，形成晚新生代的活动断层。例如，1954年民勤县东南侧发生的7级地震，刘白云等（2014）根据成丛小震发生在大震断层面附近的原则并参考前人给出极震区长轴形态，给出民勤地震的发震断层为近东西向的左行走滑断层；赵凌强等（2018）通过一条南北向的电性剖面研究，认为发震断裂位于一条高角度逆冲为主兼具左旋走滑特性的逆冲走滑断裂带，该断裂带是在青藏高原地块与阿拉善地块之间形成的一条块体边缘碰撞带，总体上阿拉善南缘晚新生代断裂系统以左行走滑兼逆冲为特征。

与南缘不同，阿拉善地块东缘的构造走向以NNE为主，活动断裂多利用了中生代期间形成的构

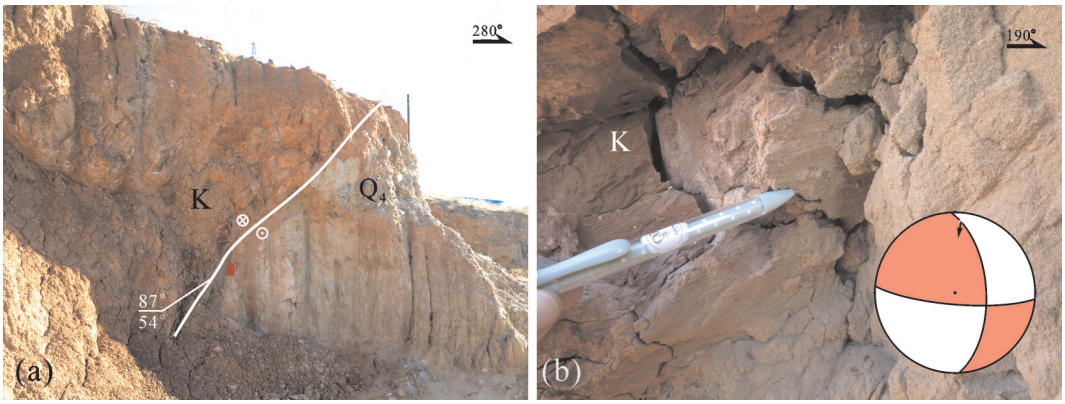

图12 阿拉善左旗市区北侧右行兼逆冲活动断层
a—断层外貌;b—断层面上发育的擦痕
Fig.12 Active reverse-dextral fault on the north side of Alxa Left Banner
a-Outcrop of fault; b-Striae on fault plane showing dextral slip with reverse slip component

造线方向(Darby et al., 2007; Yang et al., 2018)。在阿拉善地块东缘的贺兰山地区,银川盆地与贺兰山之间是一条全新世正断层,兼有右行走滑分量(邓起东等,1999),而贺兰山西缘的巴彦浩特断裂是一条右行兼有逆冲的全新世活动断裂,全新世以来的右行走滑距离达到800 m(雷启云等,2017)。在阿拉善左旗巴彦浩特北侧,见到白垩纪紫色粉砂质泥岩右行斜冲到西侧第四系之上,第四系下部为厚层均质未胶结细砂,上部为含有磨圆砾石的洪积扇沉积,时代可能为早全新世(图12a)。断层面上擦痕指示断层为右行走滑兼逆冲(图12b),与雷启云等(2017)通过水系错断得出的右行走滑一致。

在银川盆地和河套—吉兰泰盆地过渡区域,近年来记录了多次5级以上地震(图13),包括1976年6.2级地震(许忠淮等,2000)、2015年5.8级地震(韩晓明等,2015;魏建民等,2015;宋超等,2018)。2015年5.8级地震未见地表破裂,震源机制解给出的两个节面分别为近南北向和近东西向,节面陡立,断层性质为走滑(图13)。该地震震源附近多被沙漠覆盖,在震源东北侧约30 km黄河西岸巴彦木仁地区(坐标:39°59.8′N,106°38′E),发育有晚新生代密集近东西向活动正断层(图14)。断层面切穿砖红色粉砂质黏土夹中薄层细砂(时代可能为更新世),断层带顶部裂隙被第四系风成沙填充,表明断层晚第四纪活动。断面上擦痕为高角度倾滑,多数断层的断距可通过错断的地层测量,范围在几米之内,有的断层断距大于2 m(图14)。

2015年阿左旗5.8级地震的发震断层存有争议,有学者认为是近东西向的断层面左行活动导致(宋超等,2018),震源区无地表破裂可以参考。距离震源很近的巴彦木仁地区露头所见密集断层为近东西向,但断层运动学指示近南北向倾滑(图14),并无明显的左行走滑分量;另一些学者根据贺兰山东麓断裂具有右行性质,推测该地震是南北向断层面右行活动(魏建民等,2017)。地球物理资料显示磴口—本井断裂是控制河套盆地东南边界的一条NE向隐伏断裂,但震源机制解给出的节面与NE-SW走向的断裂呈一定夹角,该地震可能不是NE向隐伏断裂活动导致,因此对于发震断层的确定还需进一步结合区域构造背景。

河套盆地和银川盆地附近小震震源机制解以及GPS速度场表明,地块周边区域应力场以水平作用为主。阿拉善东缘P轴平均方位为NE-SW或NEE-SWW向,T轴方位NW-SE向(范俊喜等,2003;韩晓明等,2015)。此外地应力、断层滑动矢量数据表明该区最大主压应力方位为NE向(Heidbach et al., 2016)。巴彦浩特断裂右行走滑(图12)指示贺兰山西缘遭受NE-SW方向的最大主压应力,同时河套盆地和银川盆地之间的千里山—岗德尔山山前断裂性质为正断兼右行走滑(Liang et al., 2019)。银川盆地两侧断裂都具有右行走滑分量。控制河套盆地的断裂为NE向的狼山山前断裂以及隐伏的磴口—本井断裂,受NW-SE向拉张断裂近倾滑活动。两个盆地之间通过乌海盆地两侧近南北向断裂相连,形成连接盆地的转

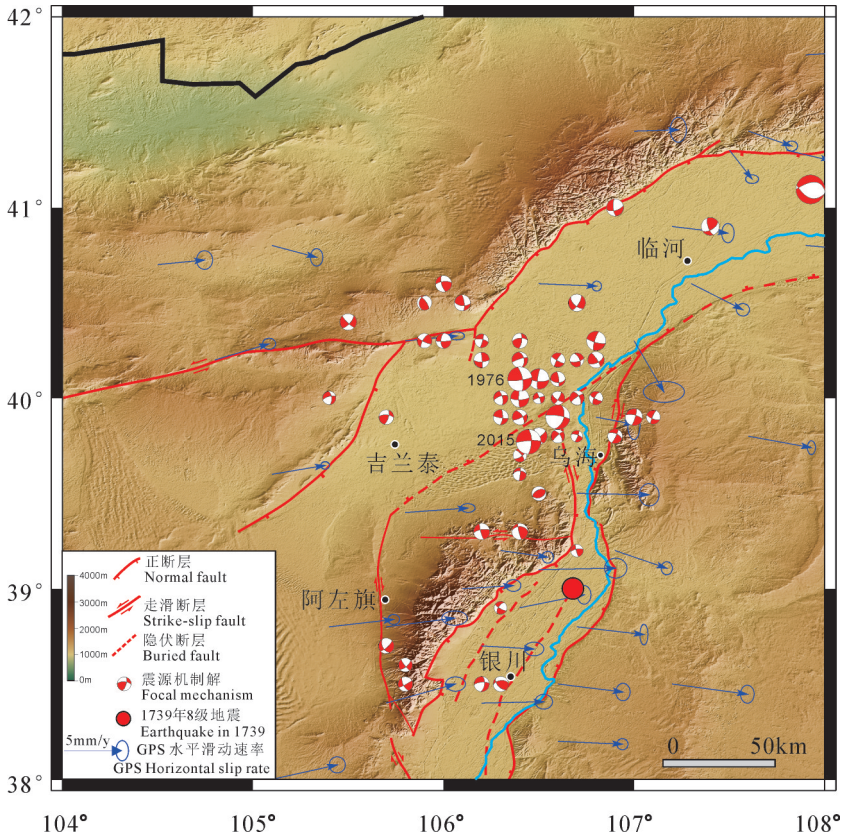

图13 河套盆地和银川盆地震源机制解及地应力方位(震源数据引自高熹微等,2015;GPS速度场引自Zhao et al., 2017)

Fig.13 Focal mechanisms and GPS velocity field in Jilantai −Hetao basin and Yinchuan basin (earthquake data from Gao et al., 2015; GPS velocity field from Zhao et al., 2017)

换构造(Morley et al., 1990; Gawthorpe and Hurst, 1993; Faulds and Varga, 1998),河套盆地—银川盆地之间通过右行走滑断裂调节两个盆地的伸展,即乌海附近黄河两岸的断层性质具有右行走滑分量,调节两个盆地NW−SE向的伸展(图15)。推测该区域发生的5级以上地震断层与黄河东岸的断层类似,处于两个盆地之间的调节带,是近南北向断层右行活动所致。巴彦木仁地区的近东西向正断层具有断距小、密集分布特征,可能是南北向走滑断层端部的次级断层。

6 结 论

(1)狼山地区新生代以来经历多期次构造活动,分别为中新世NW−SE向挤压,NNE−SSW向挤压和NW−SE向伸展,狼山地区的3期断层与青藏高原东北缘的逐步扩展以及应力场调整有关。

(2)狼山山前正断层前期通过多条断层连接,

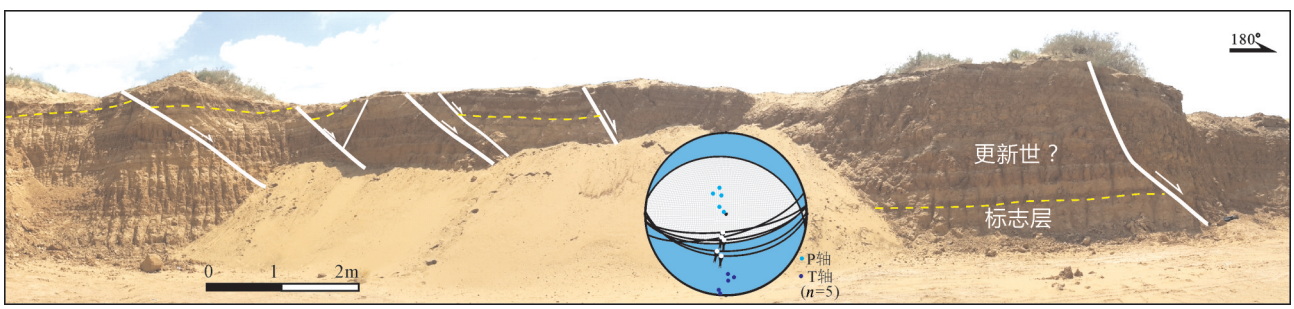

图14 乌海市北侧巴彦木仁地区东西向活动正断层

Fig.14 EW−striking normal faults in Bayanmuren area on the north side of Wuhai City

图15 河套—吉兰泰断陷与银川断陷空间关系示意图
Fig.15 Block diagram showing the spatial relation between Jialantai−Hetao basin and Yinchuan basin

目前贯通为一条断层,基本符合恒定长度演化模型,最大滑动速率和最大位移值位于断层中部。不同分段的断层滑动速率预测值与实际观测值趋势较为一致,并且全新世以来断层滑动速率可能有减缓的趋势。

(3)河套—吉兰泰盆地和银川盆地属于两个性质不同的伸展盆地,受现今NE−SW挤压构造应力状态控制,前者以近纯伸展为主,后者伸展同时带有右行走滑分量。两个盆地之间发育转换带,在NE−SW挤压构造应力作用下,转换带内地震活动可能是右行走滑所致。

致谢: 南京大学张庆龙教授对初稿给出详细意见,兰州乐途汽车租赁有限公司张新义在野外给予热心帮助,光释光样品测试得到地震局地壳应力研究所赵俊香博士大力支持。两位审稿专家给出具体宝贵修改意见,在此一并表示感谢。

注释

❶宁夏回族自治区地质局区域地质测量队. 1980. 中华人民共和国地质图(1: 20万磴口县幅区域地质调查报告).

References

Burchfiel B C, Zhang P, Wang Y, Song F, Deng Q, Molnar P, Royden L. 1991. Geology of the Haiyuan fault zone, Ningxia− Hui Autonomous Region, China, and its relation to the evolution of the northeastern margin of the Tibetan Plateau[J]. Tectonics, 10(6): 1091−1110.

Chen Fahu, Fan Yuxin, Chun Xi, Madsen D B, Oviatt C G, Zhao Hui, Yang Liping, Sun Yang. 2008: Preliminary research on Megalake Jilantai− Hetao in the arid areas of China during the Late Quaternary[J]. Chinese Science Bulletin, 53(11): 1725−1739.

Chen Lichun, Ran Yongkang, Yang Xiaoping. 2003. Late Quaternary activity and segmentation model of the Seertengshan Piedmont fault[J]. Earthquake Research in China, 19(3):255−265(in Chinese with English abstract).

Choi J H, Klinger Y, Ferry M, Ritz J F, Kurtz R, Magali R, Laurent B, Battogtokh B, Nyambayar, Sodnomsambuu R. 2018. Geologic inheritance and earthquake rupture processes: The 1905 M≥ 8 Tsetserleg− Bulnay strike− slip earthquake sequence, Mongolia[J]. Journal of Geophysical Research: Solid Earth, 123(2): 1925−1953.

Clark M K, Farley K A, Zheng D, Wang Z, Duvall A R. 2010. Early Cenozoic faulting of the northern Tibetan Plateau margin from apatite (U−Th)/He ages[J]. Earth & Planetary Science Letters, 296 (1/2):78−88.

Cowie P A, Roberts G P. 2001. Constraining slip rates and spacings for active normal faults[J]. Journal of Structural Geology, 23(12): 1901−1915.

Crone A J, Haller K M. 1991. Segmentation and the coseismic behavior of Basin and Range normal faults: Examples from east−central Idaho and southwestern Montana, USA[J]. Journal of Structural Geology, 13(2): 151−164.

Cui X, Zhao Q, Zhang J, Wang Y, Zhang B, Nie F, Qu J, Zhao H. 2018. Late Cretaceous−Cenozoic multi−stage denudation at the western Ordos block: Constraints by the apatite fission track dating on the Langshan[J]. Acta Geologica Sinica, 92(2): 536−555.

Cunningham W D, 1998. Lithospheric controls on late Cenozoic construction of the Mongolian Altai[J]. Tectonics, 17(6): 891−902.

Cunningham D. 2013. Mountain building processes in intracontinental oblique deformation belts: Lessons from the Gobi Corridor, Central Asia[J]. Journal of Structural Geology, 46: 255−282.

Dan W, Li X H, Wang Q, Wang X C, Wyman D A, Liu Y. 2016. Phanerozoic amalgamation of the Alxa Block and North China Craton: evidence from Paleozoic granitoids, U−Pb geochronology and Sr− Nd− Pb− Hf− O isotope geochemistry[J]. Gondwana Research, 32: 105−121.

Darby B J, Ritts B D. 2007. Mesozoic structural architecture of the Lang Shan, North−Central China: Intraplate contraction, extension, and synorogenic sedimentation[J]. Journal of Structural Geology, 29 (12): 2006−2016.

Dawers N H, Anders, M H. 1995. Displacement− length scaling and fault linkage[J]. Journal of Structural Geology, 17(5): 607611−609614.

Deng Qidong, Cheng Shaoping, Min Wei, Yang Guizhi, Ren dianwei. 1999. Discussion on Cenozoic tectonics and dynamics of Ordos block[J]. Journal of Geomechanics, 5:13− 21(in Chinese with English abstract).

Ding Guoyu. 1995. The segmentation model of active fault[J]. Earth Science Frontiers, (2):195−202(in Chinese with English abstract).

Dong Shaopeng. 2016. Late Quaternary Tectonic Activity and Paleoseismology along the Langshan Range− front Fault[D]. Institute of Geology, China Earthquake Administrator.

Dong S, Zhang P, Zhang H, Zheng W, Chen, H. 2018a. Drainage Responses to the Activity of the Langshan Range−Front Fault and Tectonic Implications[J]. Journal of Earth Science, 29(1): 193−209.

Dong S, Zhang P, Zheng W, Yu Z, Lei Q, Yang H, Liu J, Gong H, 2018b. Paleoseismic observations along the Langshan range−front fault, Hetao Basin, China: Tectonic and seismic implications[J]. Tectonophysics, 730: 63−80.

DuRoss C B, Personius S F, Crone A J, Olig S S, Hylland M D, Lund W R, Schwartz D P. 2016. Fault segmentation: New concepts from the Wasatch Fault Zone, Utah, USA[J]. Journal of Geophysical Research−Solid Earth, 121(2): 1131−1157.

Duvall A R, Clark M K, Kriby E, Farley K A, Craddock W H, Li C, Yuan D. 2013. Low− temperature thermochronometry along the Kunlun and Haiyuan Faults, NE Tibetan Plateau: Evidence for kinematic change during late−stage orogenesis[J]. Tectonics, 32(5): 1190−1211.

Fan Junxi, Ma Jin, Diao Guiling. 2003. Contemporary tectonic stress filed around the Ordos fault block inferred from earthquake focal mechanism[J]. Seismology Geology, 25: 88− 99(in Chinese with English abstract).

Fang X, Garzione C, Van der Voo R, Li J, Fan M. 2003. Flexural subsidence by 29 Ma on the NE edge of Tibet from the magnetostratigraphy of Linxia Basin, China[J]. Earth and Planetary Science Letters, 210(3): 545−560.

Feng J Y, Xiao W J, Windley B, Han C M, Wan B, Zhang J, Ao S J, Zhang, Z Y, Lin L N. 2013. Field geology, geochronology and geochemistry of mafic− ultramafic rocks from Alxa, China: Implications for Late Permian accretionary tectonics in the southern Altaids[J]. Journal of Asian Earth Sciences, 78: 114−142.

Feng L X, Brown R W, Han B F, Wang Z Z, Luszczak K, Liu B, Zhang Z C, Ji J Q. 2017. Thrusting and exhumation of the southern Mongolian Plateau: Joint thermochronological constraints from the Langshan Mountains, western Inner Mongolia, China[J]. Journal of Asian Earth Sciences, 144: 287−302.

Faulds James E, Varga Robert J. 1998. The role of accommodation zones and transfer zones in the regional segmentation of extended terranes[J]. Geological Society of America Special Papers, 323: 1−45.

Fossen H, Rotevatn A. 2016. Fault linkage and relay structures in extensional settings—A review[J]. Earth− Science Reviews, 154: 14−28.

Gawthorpe R L, Hurst J Mo. 1993. Transfer zones in extensional basins: their structural style and influence on drainage development and stratigraphy[J]. Journal of the Geological Society, 150(6): 1137−1152.

Gao Xiwei, Wan Yongge, Huang Jichao, Li Xiang, Cui Huawei. 2015. Tectonic stress field analysis and static coulomb stress changes of the Ms5.8 Inner Mongolias Alxa Left Banner Earthquake[J]. North China Earthquake Sciences, 33(2), 48−54(in Chinese with English abstract).

Gong Wangbin, Hu Jianmin, Li Zhenhong, Wu Sujuan, Liu Yang, Yan Jiyuan, 2013. The sediment features of lower piedmont platforms along Western Hetao Basin and implication for subsiding process and controlling factors of "Jilantai−Hetao" Megalake[J]. Earth Sci. Front, 20 (4): 190−198(in Chinese with English abstract).

Han Xiaoming, Liu Fang, Hu Bo, Zhang Fan.2015. Space− Time Distribution Characteristics of the focal mechanism type in Hetao seismic belt[J]. Journal of Jilin University: Earth Science Edition,45 (2):592−601(in Chinese with English abstract).

He C Q, Cheng Y L, Rao G, Chen P, Hu J M, Yu Y L, Yao Q. 2018. Geomorphological signatures of the evolution of active normal faults along the Langshan Mountains, North China[J]. Geodinamica Acta, 30(1): 163−182.

He X L, Zhang X J, He Z X, Jia L Y, Ye P S, Zhao J X. 2017. Late Quaternary alluvial fan terraces: Langshan, Inner Mongolia, China[J]. Geomorphology, 286: 34−44.

Heidbach O, Rajabi M, Reiter K, Ziegler M, WSM team. 2016. World stress map database release 2016[BD]. GFZ Data Services.

He Zexin, Zhang Xujiao, Jia Liyun, Wu Fadong, Zhou Yiqun, Bao Shuyan, Bao Zhiqiang, Yin Zhigang, Guo Bin. 2014. Genesis of piedmont terraces and its Neotectonic movement significance in Langshan Mountain area, Inner Mongolia[J]. Geoscience 28 (1): 98−108 (in Chinese with English abstract).

Hu J M, Gong W B, Wu S J, Liu Y, Liu S C. 2014. LA− ICP− MS zircon U−Pb dating of the Langshan Group in the northeast margin of the Alxa block, with tectonic implications[J]. Precambrian Research, 255: 756−770.

Jia L, Zhang X, He Z, He X, Wu F, Zhou Y, Fu L, Zhao J. 2015. Late Quaternary climatic and tectonic mechanisms driving river terrace development in an area of mountain uplift: A case study in the Langshan area, Inner Mongolia, northern China[J]. Geomorphology, 234: 109−121.

Jia L, Zhang X, Ye P, Zhao X, He Z, He X, Zhou Q, Li J, Ye M., Wang Z, Meng J. 2016. Development of the alluvial and lacustrine terraces on the northern margin of the Hetao Basin, Inner Mongolia, China: Implications for the evolution of the Yellow River in the Hetao area since the Late Pleistocene[J]. Geomorphology, 263: 87−98.

Jiang Wali. 2002. Paleo− earthquake event and co− seismic vertical deformation recognition along the Langshan−Sertenshan Pediment Fault, Inner Mongolia[C]//Collections of Crustal Tectonics and Crustal Stress 15, 45−52(in Chinese with English abstract).

Jolivet M, Brunel M, Seward D, Xu Z, Yang J, Roger F, Tapponnier P, Malavieille J, Arnaud N, Wu C. 2001. Mesozoic and Cenozoic tectonics of the northern edge of the Tibetan plateau: fission−track constraints[J]. Tectonophysics, 343(1/2): 111−134.

Lei Q Y, Zhang P Z, Zheng W J, Chai C Z, Wang W T, Peng D, Yu J X. 2016. Dextral strike− slip of Sanguankou− Niushoushan fault zone and extension of arc tectonic belt in the northeastern margin of the Tibet Plateau[J]. Science China Earth Sciences, 59(5): 1−16.

Lei Qiyun, Zhang Peizhen, Zheng Wenjun, Chai Chizhang, Wang Weitao, Du Peng, Yu Jingxing. 2017.Geological and geomorphic evidence for dextral strike slip of the Helanshan west− Piedmont Fault and its tectonic implications[J]. Seimology and Geology, 39 (6): 1297−1315 (in Chinese with English abstract).

Li Yanbao Ran Yongkang, Chen Lichun, Wu Fuyao, Lei Shengxue. 2015. The latest surface rupture events on the major active faults and great historical earthquakes in Hetao fault−depression zone[J]. Seismology Geology, 37(1):110− 125 (in Chinese with English abstract).

Liang K, Ma B, Li D, Tian Q, Sun C, He Z, Zhao J, Liu R,Wang J. 2019. Quaternary activity of the Zhuozishan West Piedmont Fault provides insight into the structural development of the Wuhai Basin and Northwestern Ordos Block, China[J]. Tectonophysics, 754: 56−72.

Liang Shiming, Gan Weijun, Shen Chuanzheng, Xiao Genru, Liu Jing, Chen Weitao, Ding Xiaoguang, Zhou Deming. 2013. Three−dimensional velocity field of present− day crustal motion of the Tibetan Plateau derived from GPS measurements[J]. Journal of Geophysical Research: Solid Earth, 118(10): 5722−5732.

Liu Baiyun, Zeng Wenhao, Yuan Daoyang, Chen Wenkai, Niu Yanping. 2014. Fault parameters and slip properties of the 1954 northern Tengger desert M7.0 earthquake[J]. China Earthquake Engineering Journal, 36(3): 622− 627(in Chinese with English abstract) .

Liu X B, Hu J M, Shi W, Chen H, Yan J Y. 2019. Palaeogene−Neogene sedimentary and tectonic evolution of the Yinchuan Basin, western North China Craton[J]. International Geology Review, 1−19.

Maniatis G, Hampel A. 2008, Along− strike variations of the slip direction on normal faults: Insights from three−dimensional finite−element models[J]. Journal of Structural Geology, 30(1):21−28.

Manighetti I, Caulet C, Barros L, Perrin C, Cappa F, Gaudemer Y. 2015. Generic along− strike segmentation of Afar normal faults, East Africa: Implications on fault growth and stress heterogeneity on seismogenic fault planes[J]. Geochemistry, Geophysics, Geosystems, 16(2): 443−467.

Meyer B, Tapponnier P, Bourjot L, Me´tivier F, Gaudemer Y, Peltzer G, Guo S, Chen Z. 1998. Crustal thickening in Gansu− Qinghai, lithospheric mantle subduction, and oblique, strike− slip controlled growth of the Tibet plateau[J]. Geophysical Journal International, 135(1): 1−47.

Middleton T A, Walker R T, Rood D H, Rhodes E J, Parsons B, Lei Q, Elliott J R, Zhou Y. 2016. The tectonics of the western Ordos Plateau, Ningxia, China: Slip rates on the Luoshan and East Helanshan Faults[J]. Tectonics, 35(11):2754−2777.

Molnar P, Tapponnier P. 1975. Cenozoic tectonics of Asia: Effects of a continental collision[J]. Science, 189(4201): 419−426.

Molnar P, Tapponnier P. 1977. Relation of the tectonics of eastern China to the India−Eurasia collision: Application of slip−line field theory to large−scale continental tectonics[J]. Geology, 5(4): 212−216.

Morley C K, Nelson R A, Patton T L, Munn S G. 1990. Transfer zones in the East African rift system and their relevance to hydrocarbon exploration in rifts [J]. AAPG Bulletin, 74(8): 1234−1253.

Murray A S, Wintle A G. 2003. The single aliquot regenerative dose protocol: potential for improvements in reliability[J]. Radiation Measurements, 37(4/5): 377−381.

Peng Runmin, Zhai Yusheng, Wang Jianping, Chen Xifeng, Liu Qiang, Lu Junyang, Shi Yongxing, Wang Gang, Li Shenbin, Wang Ligong, Ma Yutao, Zhang Peng. 2010. Discovery of Neoproterozoic acid volcanic rock in the southwestern section of Langshan, Inner Mongolia[J]. Chinese Science Bulletin, 55(26), 2611− 2620 (in Chinese with English abstract).

Ran Yongkang, Chen Lichun, Yang Xiaoping, Han Zhujun. 2003. Recurrence characteristic of late Quaternary strong earthquakes on the major faults along the northern border of Ordos block[J]. Science China(Serious D): Earth Science 46 (2 Suppl.), 189− 200 (in Chinese with English abstract).

Rao G, Chen P, Hu J, Yu Y, Qiu J. 2016. Timing of Holocene paleo−earthquakes along the Langshan Piedmont Fault in the western Hetao Graben, North China: Implications for seismic risk[J]. Tectonophysics, 677: 115−124.

Rao Gang, He Chuanqi, Cheng Yali, Yu Yangli, Hu Jianmin, Chen Peng, Yao Qi. 2018. Active normal faulting along the Langshan Piedmont Fault, North China: Implications for slip partitioning in the western Hetao Graben[J]. The Journal of Geology, 126(1): 99−118.

Research Group of Active Fault System around the Ordos Massif.1988. Active Fault System Around Ordos Massif[M]. Beijing: Seismological Press, 39− 65(in Chinese with English abstract).

Rotevatn A, Jackson C A L, Tvedt A B M, Bell R E, Blækkan I. 2019. How do normal faults grow?[J]. Journal of Structural Geology, 125: 174−184.

Schultz R A. 1997. Displacement− length scaling for terrestrial and Martian faults: Implications for Valles Marineris and shallow planetary grabens[J]. Journal of Geophysical Research: Solid Earth, 102(B6): 12009−12015.

Shen X, Li D, Tian Y T, Lv Y W, Li D W, Li Y F. 2016. Late Pleistocene− Holocene slip history of the Langshan− Seertengshan piedmont fault (Inner Mongolia, northern China) from cosmogenic ^{10}Be dating on a bedrock fault scarp[J]. Journal of Mountain Science, 13(5): 882−890.

Schwartz D P, Coppersmith K J. 1984. Fault behavior and characteristic earthquakes: Examples from the Wasatch and San Andreas fault zones[J]. Journal of Geophysical Research: Solid Earth, 89(B7): 5681−5698.

Shi W, Dong S, Liu Y, Hu J, Chen X, Chen P. 2015. Cenozoic tectonic evolution of the South Ningxia region, northeastern Tibetan Plateau inferred from new structural investigations and fault kinematic analyses[J]. Tectonophysics, 649: 139−164.

Song Chao, Gai Zengxi. 2018. An iterative travel time inversion and waveform modeling method to determine the crust structure and the focal mechanism of 2015 Alxa Left Banner Ms5.8 Earthquake[J]. Chinese Journal of Geophysics, 61(4):1225− 1237 (in Chinese with English abstract).

Tapponnier P, Molnar P. 1976. Slip− line field theory and large− scale

continental tectonics[J]. Nature, 264(5584):319−324.

Tapponnier P, Peltzer G, Dain A Y L, Armijo R, Cobbold. 1982. Propagating extrusion tectonics in Asia: New insights from simple experiments with plasticine[J]. Geology, 10(10):611.

Tapponnier P, Zhiqin X, Roger F, Meyer B, Arnaud N, Wittlinger G, Jingsui Y. 2001 Oblique stepwise rise and growth of the Tibet Plateau[J]. Science, 294(5547): 1671−1677.

Wang W, Kirby E, Peizhen Z, Dewen Z, Guangliang Z, Huiping Z, Wenjun Z, Chizhang C. 2013. Tertiary basin evolution along the northeastern margin of the Tibetan Plateau: Evidence for basin formation during Oligocene transtension[J]. Geological Society of America Bulletin, 125(3/4): 377−400.

Wang Xulong, Lu yanchou, Li Xiaoni. 2005. Luminescence dating of fine−grained quartz in Chinese Loess simplified Multiple Aliquot Regenrative−Dose(MAR) Protocol[J]. Seismology Geology, 27(4): 615−623 (in Chinese with English abstract).

Wei Jianmin, Han Xiaoming, Zhang Fan, Chen Lifeng, Li Juan, Yang Hongying. 2017. Discussion of the earthquake sequence and earthquake rupture surface of Alxa Zuoqi Ms5.8 in 2015[J]. China Earthquake Engineering Journal, 39(5): 919−924 (in Chinese with English abstract).

Wu Weimin, Nie Zongsheng, Xu Guilin.1996. Active faulting research on west segment of Serteng rangefront fault [C]//Institute of Geology, SSB(ed.). Research on Active Faults(5). Beijing: Seismological Press, 113−124(in Chinese with English abstract).

Xu Zhonghuai, Wang Suyun, Gao Ajia. 2000. Present−day tectonic movement in the northeastern margin of the Qinghai−Xizang (Tibetan) Plateau as revealed by earthquake activity[J]. Acta Seismologica Sinica,22(5):472− 481(in Chinese with English abstract).

Yang Xiangyang, Dong Yunpeng. 2018. Mesozoic and Cenozoic multiple deformations in the Helanshan Tectonic Belt, Northern China[J]. Gondwana Research, 60: 34−53.

Yin A, Nie S Y. 1996. A Phanerozoic Palinspastic Reconstruction of China and its Neighboring Regions[C]//An Yin and Harrison T M (eds.). The Tectonic Evolution of Asia. Cambridge University Press, 442−485.

Yin A. 2010. Cenozoic tectonic evolution of Asia: A preliminary synthesis[J]. Tectonophysics, 488(1/4):293−325.

Yu J X, Zheng W J, Kirby E, Zhang P Z, Lei Q Y, Ge W P, Wang W T, Li X N, Zhang, N. 2016. Kinematics of late Quaternary slip along the Yabrai fault: Implications for Cenozoic tectonics across the Gobi Alashan block, China[J]. Lithosphere, 8(3): 199−218.

Yu J X, Zheng W J, Zhang P Z, Lei Q Y, Wang X L, Wang W T, Li X N, Zhang N. 2017. Late Quaternary strike−slip along the Taohuala Shan−Ayouqi fault zone and its tectonic implications in the Hexi Corridor and the southern Gobi Alashan, China[J]. Tectonophysics, 721:28−44.

Yuan Daoyang, Zhang Peizhen, Liu Baichi, Gan Weijun, Mao Feng Yiing, Wang Zhicai, Zheng Wenjun, Guo Hua. 2004. Geometrical imagery and tectonic transformation of Late Quaternary active tectonics in northeastern margin of Qinghai−Xizang Plateau[J]. Acta Geologica Scinca, 78(2):270−278 (in Chinese with English abstract).

Yuan D Y, Ge W P, Chen Z W, Li C Y, Wang Z C, Zhang, H P, Zhang P Z, Zheng D W, Zheng W J, Craddock W H, Dayem K E, Duvall A R, Hough B G, Lease R O, Champagnac J D, Burbank D W, Clark M K, Farley K A, Garzione C N, Kirby E, Molnar P, Roe G H. 2013. The growth of northeastern Tibet and its relevance to large−scale continental geodynamics: A review of recent studies[J]. Tectonics, 32(5): 1358−1370.

Zhang H, He Z, Ma B, Long J, Liang K, Wang J. 2017. The vertical slip rate of the Sertengshan piedmont fault, Inner Mongolia, China[J]. Journal of Asian Earth Sciences, 143:95−108.

Zhang J, Cunningham D, Hongyi C. 2010. Sedimentary characteristics of Cenozoic strata in central−southern Ningxia, NW China: Implications for the evolution of the NE Qinghai−Tibetan Plateau[J]. Journal of Asian Earth Sciences, 39(6): 740−759.

Zhang J, Li J, Xiao W, Wang Y, Qi W. 2013. Kinematics and geochronology of multistage ductile deformation along the eastern Alxa block, NW China: New constraints on the relationship between the North China Plate and the Alxa block[J]. Journal of Structural Geology, 57(57):38−57.

Zhang J, Li J, Li Y, Qi, W., Zhang, Y. 2014. Mesozoic−Cenozoic multi−stage intraplate deformation events in the Langshan Region and their Tectonic Implications[J]. Acta Geologica Sinica, 88(1): 78−102.

Zhang P, Burchfiel B C, Molnar P, Zhang W, Jiao D, Deng Q, Wang Y, Royden L, Song F. 1991. Amount and style of Late Cenozoic deformation in the Liupan Shan area, Ningxia Autonomous Region, China[J]. Tectonics, 10(6): 1111−1129.

Zhang Yueqiao, Liao Changzhen, Shi Wwi, Hu Bo. 2006. Neotectonic evolution of the peripheral zones of the Ordos basin and geodynamic setting[J]. Geological Journal of China Universities, 12:285−297(in Chinese with English abstract).

Zhang Y Q, Mercier J L, Vergély P. 1998. Extension in the graben systems around the Ordos (China), and its contribution to the extrusion tectonics of south China with respect to Gobi−Mongolia[J]. Tectonophysics, 285(1): 41−75.

Zhao B, Zhang C, Wang D, Huang Y, Tan K, Du R, Liu J. 2017. Contemporary kinematics of the Ordos block, North China and its adjacent rift systems constrained by dense GPS observations[J]. Journal of Asian Earth Sciences, 135: 257−267.

Zhao Heng, Zhang Jin, Qu Junfeng, Zhang Beihang, Niu Pengfei, Hui Jie, Yun Long, Li Yanfeng, Wang Yannan, Zhang Yiping. 2019a. Characteristics and Dynamic Background of the Cenozoic Compressive Structures in the Eastern Margin of the Alxa Block[J]. Earth Science. doi:10.3799/dgkx.2019.126.

Zhao Heng, Zhang Jin, Li Yanfeng, Qu Junfeng, Zhang Beihang, Niu Pengfei, Yun Long, Zhang Yiping, Wang Yannan. 2019b. Relay structures and linkage characteristics of normal fault:An example from the Langshan piedmont normal fault zone[J]. Acta Geologica

Sinica, 93(7):1601−1617(in Chinese with English abstract).

Zhao Lingqiang, Zhan Yan, Wang Qinglaing, Sun Xiangyu, Yang Hao, Chen Xiaobin. 2018. Deep electrical structure beneath the 1954 Ms 7.0 Minqin, Gansu earthquake and its seismotectonic environment[J]. Seismology Geology, 40(3): 552− 565(in Chinese with English abstract).

Zheng D, Zhang P Z, Wan J, Yuan D, Li C, Yin G, Chen J. 2006. Rapid exhumation at~ 8 Ma on the Liupan Shan thrust fault from apatite fission− track thermochronology: Implications for growth of the northeastern Tibetan Plateau margin[J]. Earth and Planetary Science Letters, 248(1): 198−208.

Zheng D W, Clark M K, Zhang P Z, Zheng W, Farley K A. 2010. Erosion, fault initiation and topographic growth of the North Qilian Shan (northern Tibetan Plateau) [J].Geosphere, 6(6):937−941.

Zheng Wenjun, Yuan Daoyang, Zhang Peizhen, Yu Jingxing, Lei Qiyun, Wang Weitao, Zheng Dewen, Zhang Huiping, Li Xinnan, Li Chuanyou, Liu Xingwang. 2016. Tectonic geometry and kinematic dissipation of the active faults in the northeastern Tibetan Plateau and their implications for understanding northeastward growth of the plateau[J]. Quaternary Sciences,36(4):775−788.

附中文参考文献

陈立春, 冉勇康, 杨晓平. 2003. 色尔腾山山前断裂晚第四纪活动与破裂分段模型[J]. 中国地震, 19(3):255−265.

丁国瑜. 1995. 活断层的分段模型[J]. 地学前缘, (2):195−202.

邓起东, 程绍平, 闵伟, 杨桂枝, 任殿卫. 1999. 鄂尔多斯块体新生代构造活动和动力学的讨论[J]. 地质力学学报, 5(3): 13−21.

董绍鹏. 2016. 狼山山前断裂的晚第四纪活动习性与古地震研究[D]. 中国地震局地质研究所.

国家地震局鄂尔多斯周缘断裂系课题组.1988. 鄂尔多斯周缘断裂系[M]. 北京: 地震出版社, 39− 65.

范俊喜, 马瑾, 刁桂苓. 2003. 由小震震源机制解得到的鄂尔多斯周边构造应力场[J]. 地震地质, 25(1): 88−99.

高熹微, 万永革, 黄骥超, 李祥, 崔华伟. 2015. 内蒙古阿拉善左旗M_S5.8地震的构造应力场和静态库伦应力变化分析[J]. 华北地震科学, 33(2), 48−54.

公王斌, 胡健民, 李振宏,吴素娟, 刘洋, 阎纪元. 2013. 河套盆地西缘山前低台地沉积特征对“吉兰泰—河套”古湖消退过程及其控制因素的指示意义[J]. 地学前缘, 20(4): 190−198.

韩晓明, 刘芳, 胡博, 张帆. 2015. 河套地震带的震源机制类型时空分布特征[J]. 吉林大学学报: 地球科学版, (2): 592−601.

何泽新, 张绪教, 贾丽云, 武法东, 周轶群, 鲍淑燕, 包智强, 殷志刚,郭斌. 2014. 内蒙古狼山山前台地成因及其新构造运动意义[J]. 现代地质, (1): 98−108.

江娃利. 2002. 内蒙狼山—色尔腾山山前活动断裂古地震事件识别及同震垂直位移[C]//地壳构造与地壳应力文集(15):45−52.

雷启云, 张培震, 郑文俊, 杜鹏, 王伟涛, 俞晶星, 谢晓峰. 2017. 贺兰山西麓断裂右旋走滑的地质地貌证据及其构造意义[J]. 地震地质, 39(6): 1297−1315.

李彦宝, 冉勇康, 陈立春, 吴富峣, 雷生学. 2015. 河套断陷带主要活动断裂最新地表破裂事件与历史大地震[J]. 地震地质, 37(1): 110−125.

刘白云, 曾文浩, 袁道阳, 陈文凯, 牛延平. 2014. 1954 年腾格里沙漠北 7 级地震断层面参数和滑动性质研究[J]. 地震工程学报, 36 (3): 622−627.

彭润民, 翟裕生, 王建平, 陈喜峰, 刘强, 吕军阳, 石永兴, 王刚, 李慎斌,王立功, 马玉涛, 张鹏. 2010. 内蒙狼山新元古代酸性火山岩的发现及其地质意义[J]. 科学通报, (26): 2611−2620.

冉勇康, 陈立春, 杨晓平, 韩竹军. 2003. 鄂尔多斯地块北缘主要活动断裂晚第四纪强震复发特征[J]. 中国科学: D 辑, 33(B04): 135−143.

宋超, 盖增喜. 2018. 利用走时和波形拟合迭代反演阿拉善地壳速度结构及 2015 年阿拉善左旗 5.8 级地震震源机制[J]. 地球物理学报, 61(4): 1225−1237.

王旭龙, 卢演俦, 李晓妮, 2005. 细颗粒石英光释光测年:简单多片再生法[J]. 地震地质, 27(4):615−623.

魏建民, 韩晓明, 张帆, 陈立峰, 李娟, 杨红樱. 2017. 2015 年阿拉善左旗 MS5. 8 地震序列特征及发震破裂面讨论[J]. 地震工程学报, 39(5): 919−924.

吴卫民, 聂宗笙, 许桂林.1996. 色尔腾山山前断裂西段活断层研究[C]//中国地震局地质研究所编.活动断裂研究(5).北京: 地震出版社: 13−124.

许忠淮, 汪素云,高阿甲. 2000. 地震活动反映的青藏高原东北地区现代构造运动特征[J]. 地震学报, 22(5): 472−481.

袁道阳, 张培震, 刘百篪, 甘卫军, 毛凤英, 王志才, 郑文俊, 郭华. 2004. 青藏高原东北缘晚第四纪活动构造的几何图像与构造转换[J]. 地质学报, 78(2):270−278.

张岳桥, 廖昌珍, 施炜, 胡博. 2006. 鄂尔多斯盆地周边地带新构造演化及其区域动力学背景[J].高校地质学报, 12(3):285−297.

赵衡, 张进, 曲军峰, 张北航, 牛鹏飞, 惠洁, 云龙, 李岩峰, 王艳楠, 张义平. 2019a. 阿拉善地块东缘新生代中新世挤压变形及动力学背景[J/OL]. 地球科学 .doi: 10.3799/dqkx.2019.126.

赵衡, 张进, 李岩峰, 曲军峰, 张北航, 牛鹏飞, 云龙, 张义平, 王艳楠. 2019b. 正断层的阶区构造及生长机制:以狼山山前断层带为例[J]. 地质学报, 93(7):1601−1617.

赵凌强, 詹艳, 王庆良, 孙翔宇, 杨皓, 陈小斌. 2018. 1954 年甘肃民勤7级地震区深部电性结构特征及地震构造环境研究[J]. 地震地质, 40(3): 552−565.

郑文俊, 袁道阳, 张培震, 俞晶星, 雷启云, 王伟涛, 郑德文, 张会平, 李新男, 李传友, 刘兴旺. 2016. 青藏高原东北缘活动构造几何图像、运动转换与高原扩展[J]. 第四纪研究, 36(4):775−788.